UNIVERSITY OF MINNESOTA
ST. ANTHONY FALLS HYDRAULIC LABORATORY
LORENZ G. STRAUB, Director

Technical Paper No. 42, Series B

Studies of the Reduction of Pipe Friction with the Non-Newtonian Additive CMC

by
JOHN F. RIPKEN
and
MEIR PILCH

Prepared for
DAVID TAYLOR MODEL BASIN
Department of the Navy
Washington, D.C.
under
Office of Naval Research Contract Nonr 710(49)

April 1963
Minneapolis, Minnesota

UNIVERSITY OF MINNESOTA
ST. ANTHONY FALLS HYDRAULIC LABORATORY
LORENZ G. STRAUB, Director

Technical Paper No. 42, Series B

Studies of the Reduction of Pipe Friction with the Non-Newtonian Additive CMC

by
JOHN F. RIPKEN
and
MEIR PILCH

Prepared for
DAVID TAYLOR MODEL BASIN
Department of the Navy
Washington, D.C.
under
Office of Naval Research Contract Nonr 710(49)

April 1963
Minneapolis, Minnesota

PREFACE

The evaluation studies described herein were designed to better establish the remarkable friction-reducing effectiveness of dilute non-Newtonian aqueous solutions of the chemical CMC (sodium carboxymethylcellulose) for possible application to naval drag reduction problems. The studies are part of a non-Newtonian research program which the Department of Navy initiated in 1962.

CMC is one of several available commercial long-chain polymer additives which might be employed for drag reduction. These studies serve both to extend the existing data on this particular additive and to better define the rheological characterization of other additives which might be considered under the total program.

The tests discussed in this report were undertaken in the facilities of the St. Anthony Falls Hydraulic Laboratory during the period May 1962 to May 1963 and were sponsored under the Bureau of Ships Fundamental Hydromechanics Research Program of the United States Department of Navy. The program was administered by the David Taylor Model Basin and the Office of Naval Research under contract Nonr 710(49).

The authors wish to express appreciation for the many contributions of their colleague, Harry D. Purdy.

A B S T R A C T

This study extends existing data to better clarify the manner in which the addition of a small quantity of long-chain polymer chemical additive to water can remarkably reduce the frictional resistance to flow.

The material sodium carboxymethylcellulose was added to fresh water and subjected to pipe friction tests under a wide range of shear rates, additive concentration, and temperature conditions. The frictional data are characterized by application of the power law expression for non-Newtonian fluids.

CONTENTS

LIST OF SYMBOLS

du/dr - shear rate, sec^{-1}

$(du/dr)_w$ - shear rate at a wall, sec^{-1}

C - concentration of additive, per cent by weight

C_D - empirical discharge coefficient of flow meter, dimensionless

D - pipe or tube diameter, feet

$D\Delta P/4L$ or τ - unit shear stress at the wall of a pipe or tube, lb force/sq ft

f - Fanning friction factor, dimensionless

g - gravitational constant

K - consistency index as defined by Eq. (2), (lb force)(sec^n)/sq ft

K' - consistency index as defined by Eq. (3), (lb force)($sec^{n'}$)/sq ft

L - length between measuring stations of pipe or tube, feet

n - flow behavior index as defined by Eq. (2), dimensionless

n' - flow behavior index as defined by $n' = \frac{d(\ln D\Delta P/4L)}{d(\ln 8V/D)}$, dimensionless

N_{Re} - Reynolds number for Newtonian fluids, dimensionless

N'_{Re} - Reynolds number as defined by Eq. (5), dimensionless

ΔP - pressure drop, lb force/sq ft

r - radial distance, feet

V - average velocity, ft/sec

$8V/D$ - shear rate of a Newtonian fluid at the wall of a pipe or tube for laminar flow conditions, sec^{-1}

X - longitudinal distance from entrance of pipe, feet

μ - viscosity of a Newtonian fluid, lb mass/(sec)(ft)

π - 3.1416

ρ - fluid density, lb mass/cu ft

τ - unit shear stress, lb force/sq ft

L I S T O F I L L U S T R A T I O N S

STUDIES OF THE REDUCTION OF PIPE FRICTION WITH THE NON-NEWTONIAN ADDITIVE CMC

I. INTRODUCTION

Recent evidence [1, 2]* has shown that adding less than 1 per cent of certain materials to water flowing in a pipe can reduce the usual turbulent frictional head loss by as much as 70 per cent. The details of the flow mechanism which produces this reduction in loss are not well understood for the non-Newtonian fluids involved. It has been suggested [2, 3], however, that the pseudoplastic or viscoelastic properties of these mixtures or solutions are primarily due to the fibered or long-molecule character of the additive material. These unsymmetrical fluid elements in random entanglements presumably align in shearing flow, thus tending to repress turbulence, to produce eddies with relatively motionless centers, and to correspondingly reduce the energy loss of the flow. Since the flow characteristics of these power law fluids are fundamentally different from those of the better-understood Newtonian fluids, new theories, parameters, and measuring techniques are required. Development in this expanding phase of rheology has largely occurred in applications to chemical engineering where such fluids are increasingly encountered in process operations. These developments have occurred at an increasing rate in the last five years and have served to spark naval interest in possible applications of the materials to reduction of boundary resistance in naval hydrodynamic problems. Fabula [4] has made a generalized review of an application to the reduction of torpedo drag, with the conclusion that additional experiments were needed for the clarification of a number of factors. The study described herein is one phase of a general non-Newtonian research program which the Department of Navy initiated in 1962.

This report begins with a brief review of the selection and merits of the additive materials which are commercially available and presumed adaptable to naval applications. On the basis of this review the material CMC, a long-chain polymer which is the sodium salt of carboxymethylcellulose or CMC 7HSCP, was selected for the tests under this program. The report then proceeds to describe the nature of this material and to establish the mixing,

*Numbers in brackets refer to the List of References on page 29.

handling, and characterization procedures and properties for dilute water solutions.

Because the prime naval interest relates to the reduction of boundary shear, the selected material was subjected to a wide range of shearing rates with concurrent measurement of the boundary shear force. For ready comparison with existing test data and power law theories and for practical testing, these shear studies were conducted in circular, smooth-walled pipes. To achieve a wide range of flow characteristics, the studies were conducted in two sizes of circular pipes, the largest having a diameter 18 times that of the smaller.

The current data differ from existing data in that a somewhat more extensive range and more intensive coverage were given to a particular non-Newtonian fluid and the experimental data are recorded in considerable detail to permit independent evaluation. A rather detailed variation of concentration values together with a fairly detailed coverage of the laminar-turbulent transition are believed useful to future naval application studies. It is hoped that this study will also aid in defining the techniques, value ranges, and theories necessary for exploitation of the potentials of several other promising additives.

II. THE ADDITIVE MATERIAL

A. Selection and Nature of the Additive CMC

The initial activity in this program included a search of the technical literature relative to past uses of the type of materials which was believed adaptable to naval drag reduction problems. Parallel with this, the manufacturers of these materials were solicited for technical use and price data on the materials which appeared to be of interest. As a result of this screening six materials were selected as sufficiently different and seemingly practical to warrant evaluation testing in a comprehensive program. The selected materials were sodium carboxymethylcellulose or CMC 7HSCP (Hercules Powder Co.), Jaguar and Polyhall (Stein, Hall and Co.), Methocel (Dow Chemical Co.), Carbopol (B. F. Goodrich Chemical Co.) and Westco J-2 (Westco Research).

In view of the fact that the material CMC had a history of commercial use for over 20 years and had been subjected to limited rheological studies by a number of investigators over a period of years, it appeared to be the preferred selection for initiating this investigation.

Since previous studies of CMC solutions have demonstrated a marked departure from the shear characteristics of the Newtonian fluids with which most engineers are familiar, it is perhaps in order to briefly review the generalities of these shear differences. This review is aided by first graphically demonstrating in Figs. 1 and 2 the manner in which two standard common fluids act when exposed to laminar shear in a capillary tube viscosimeter. From Fig. 1, which is a plain coordinate or arithmetic plot of the shearing unit stress (τ) versus the shearing strain or rate (du/dr), it may be seen that both fluids exhibit a linear relation differing only in the increasing slope (μ) as we proceed from the thinner to the thicker fluid. By definition, fluids which possess this linearity are Newtonian and those which are non-linear are non-Newtonian. If these same data are plotted as logarithmic values, as shown in Fig. 2, the characteristics of the two standard Newtonian fluids remain linear with the slopes both unity but with the viscosity now represented by the intercept value where the abscissa scale reads unity. It is this form of log-log plot which the rheologist finds most useful for shear data analysis.

If, using solid lines, we now add to Fig. 2 the fragmentary data [5] available for CMC solutions, we will roughly define a non-linear family of curves in which the shear force or viscosity increases as the concentration of the solution increases. Most of the available data are in the middle region where the curves are fairly straight. The data of Refs. [6, 7] indicate that for the lower shear rate values a considerable curvature develops as the concentration increases. (For very low shear rates the curves should become straight with a slope of unity.) There appear to be no available CMC data covering the high shear rate values, but other non-Newtonian solutions give evidence that the curves may again tend to become parallel (unity slope) and close to the curve of the solvent medium (water).

Fluids which have the general slope characteristics of CMC as shown in Fig. 2 are known as pseudoplastic or shear thinning fluids.

It is the purpose of this study to further define these shear curves both in the laminar regime, as shown in Fig. 2, and in the departures from these curves, as transition to turbulent flow occurs. It is quite evident from Fig. 2 that CMC added to water will not reduce shear forces in the laminar regime. This study will attempt to define the regimes in which shear force benefits will be realized by the addition of CMC.

The material CMC is the sodium salt of carboxymethylcellulose and is commercially prepared by chemically treating a cellulose to form a water-soluble cellulose gum. The resulting material is known as a high molecular weight polymer and in small amounts is quite readily soluble in water. It is extensively used in a wide variety of commercial products serving principally as a thickening agent and suspension stabilizer for foods, pharmaceuticals, cosmetics, etc., and in dried films as a sizing or finish for textiles, paper, protective coatings, etc. Its usefulness stems considerably from its physiological inertness in humans for both internal and external application. Its usefulness and availability are indicated by an annual production in excess of twenty million pounds. It costs approximately 75 cents per pound.

It is commercially available as a dry powder weighing about 35+ lb per cu ft and varying in fineness, purity, and chemical formulation. The various formulations are primarily intended to afford a range of solubilities and viscosities when dissolved in water. The type selected for these studies was CMC-7HSCP, a form providing maximum viscosity per unit additive, freedom from thixotropy, and ready dispersiveness and solubility in either hot or cold water. The dry powder is somewhat hygroscopic and will absorb atmospheric moisture up to 15 or 20 per cent of its weight in humid conditions. The powder is also subject to biological fungus or mold attack but seemed to present no particular storage problem in several months of handling at room temperature in the hydraulic laboratory.

With suitable precautions the dry powder can be hydrated and brought into solution quite readily. With the selected type, viscosities of the order of 1000 times that of water can be produced in a 1.0 per cent solution by weight, with a viscosity rise to 30,000 times that of water at 2.0 per cent solution and to solid gels around 4 or 5 per cent. Since these solutions are generally considered to be rheologically pseudoplastic in the lower concentrations (not all observers agree with this) and to possess viscoelastic and thixotropic properties in the higher concentrations, the current studies were confined to concentrations of 0.0, 0.1, 0.25, 0.50, 0.75, and 1.00 per cent by weight. For all practical purposes, these dilute solutions are of essentially the same density as the solvent water and are so considered in the data treatment of this report. The influence of temperature on the viscosity is also similar to that of water, showing a decided decrease with increasing temperatures. Limited higher temperatures (to boiling) do not permanently affect the viscosity, nor does freezing.

The viscosity of dilute solutions of CMC is a maximum with neutral water and tends to decrease with either acid or alkaline pH values and with salts. In the current studies the solutions were prepared with fresh tap water and no attempt was made to evaluate a sea water solvent. Limited test data on the extent of the sea water influence on viscosity may be found in Ref. [7]. These sea water values, which are for low shear rates, indicate that, as compared to results for fresh water solutions, the reduction in viscosity was relatively small for 1 per cent solutions but was of the order of 50 per cent for more dilute concentration. Studies of sea water solutions at high rates of shear are needed.

The storage life of CMC solutions is a function of the pH, available oxygen, sunlight, temperature, and micro-biological attack. Biological attack will result in a loss of viscosity in the solution but may be arrested by addition of a suitable preservative. The storage life is satisfactory for the time span encountered in most commercial practice and should not seriously rule against its consideration for naval applications.

The foregoing material has largely been drawn from Ref. [8].

Shaver and Merrill [2] describe CMC in dilute solution as a nonassociating, free-draining, random-coiling polymer having some degree of stiffness but nonetheless quite flexible when compared with more rigid types.

B. Mixing and Handling of the Additive

While CMC is readily soluble in either hot or cold water, certain precautions are necessary in the mixing of the powder with water. The prime difficulty stems from the fact that the initial phase of solution consists of a wetting and swelling of the solid particles as hydration begins. This is followed by gradual solution. If the particles are first wetted as an aggregate mass which is not immediately broken down, a swollen tough skin forms over the surface of the mass to produce a lump which is then dispersed and dissolved with difficulty. In consequence, handling procedures should involve dispersed addition of the solids at a rate which will permit wetting exposure of the particles under active shearing conditions. The rate of addition should be slow enough to prevent lumping but fast enough to assure dispersion of the solid in the solvent before complete hydration or thickening occurs. The CMC used in these tests has a C in the suffix code indicating that the finer powder parts have been removed leaving a relatively coarse solid. While these coarser powder particles are somewhat slower in dissolving than the fine powder, they are much easier to disperse in the solvent without lumping and with active agitation they will completely dissolve in a few minutes.

In the initial studies, with small batches, mixing was accomplished with a standard kitchen mixer and bowl with the powder dusted onto the agitated liquid surface with a salt shaker under room temperature conditions. Agitation for about ten minutes then led to clear and usable solutions yielding normal viscosity values.

Preparation of solutions for the larger pipe flow facility was accomplished in a 55-gal barrel using a 400-lb water fill and a carefully weighed quantity of powder. The powder weight was corrected for hygroscopic water content based on oven-dried samples. Dispersion and mixing in the barrel were accomplished with a small centrifugal pump (H = 30 ft, Q = 20 gpm, hp = 3/4) which sucked from the bottom of the barrel and discharged into an injector (Penberthy Mfg. Co., XL-96, 3A, 1-in. size) with its suction throat opening positioned a few inches below the surface of the liquid in the barrel. Screw adjustment of the vertical position of the injector would permit a surface vortex to form with a small air-sucking core feeding into the injector throat. With a small funnel directing the powder into the vortex core, a modest rate of manual powder feed could be maintained into the pumped stream and solutions of up to 1.0 per cent could be dispersed and dissolved in less than 10 minutes under room temperature conditions. No difficulty was encountered with this pump-injector dispersion and agitation system for the more dilute solutions, but thickening occurred with the more concentrated solutions (1.00 per cent) before dispersion was completed. This led to a discharge reduction and inadequate vortex action. A pump revision doubling the output head restored the vortex strength.

An additional difficulty with the higher concentrations evolved from the inherent need for sucking a small quantity of air into the injector along with the dry powder. This entrained air had a very slow rise time and usually required several hours of settling time before the bubbles cleared.

C. Degradation and Inhibition

High molecular weight polymers of the type employed in these tests evidently consist of macro-size long-chain molecules in random, loosely-coiled entanglements. Exposure of a solution of such molecules to a sufficiently powerful shearing action can cause chain scission which permanently degrades the polymer molecular weight. This degrading action not only produces a measurable change in the chemical-physical characteristics of the material, but also changes the shear flow characteristics which are in some manner associated with the dimensional properties of the nonsymmetrical molecules.

While relatively little specific information is available on mechanical degradation it appears that all shearing, mixing, or pumping operations tend to produce some degrading effect. The most marked effects, however, have occurred where the solution has been exposed to ultrasonic irradiation involving cavitation. It is not clear whether such action is involved with the chemistry of high temperatures and pressures in the collapse region or whether it involves the high mechanical shear of the collapse shock wave.

There is some evidence to show a slight increase in the degradation as the viscosity of the solvent fluid increases. This is due to the increasing shear stressing of the chain. In consequence, since viscosity normally decreases with temperature, we may expect degradation to decrease with increasing temperature. In low pressure systems the latter effect may be countered by the increased tendency to cavitate as the temperature increases.

Concentration of the chain molecule has a strong influence on degradation, as the scission action of chain on chain is much stronger than that of solvent on chain. Accordingly, high concentrations of additive appear to afford more marked degradation evidences.

Shearing degradation data for CMC solutions were not found in the literature but somewhat related tests are, however, available in [9]. In these tests, the test fluid was sheared between a stator surface and the face of a rapidly revolving disk. The shearing conditions approximated the range of about 25,000 to 400,000 sec^{-1}. (The top shear rates of the current study were $\approx$30,000 sec^{-1}.) These tests indicate that under intense shear the molecular weight could decrease at a rate of several per cent per minute but would reduce to very small rates of change after a short time. Lesser shears involved lesser rates.

In addition to shearing degradation, degradation also occurs as the result of bacterial or enzyme action. It was assumed that spoilage degradation of this type could be inhibited by a toxic preservative, so all solutions used in these tests were chemically treated in accordance with the recommendations of the maker. The treatment consisted of the supplementary addition of the chemical sodium pentachlorophenate in a dosage which was 2 per cent by weight of the CMC solids. CMC solutions prepared in this manner were shelf stored for as long as six months without visual evidence of clouding or odor evidence of spoilage. Similar treatment of solutions used in the pipe flow facility also gave no visual or odor evidences of change for periods as long as eight weeks.

Degradation had been anticipated from the beginning of this program and, accordingly, the initial laboratory solutions were frequently evaluated with the Brookfield viscosimeter (described later) to determine any progressive viscosity change. The viscosity of the various solutions decreased less than 15 per cent in the first three weeks. In consequence the pipe test materials were only checked occasionally, following their introduction into the pipe facility. These periodic checks seemed to show little evidence of change for the tests on hydraulic gradient and wall friction even though the tests spanned a period of several weeks and involved considerable shearing exposure. However, following one of the high concentration, high velocity, high temperature Pitot tests, which involved sustained high shear for about two hours, it was noted that a marked decrease of viscosity (about 40 per cent) had occurred. It was rationalized that audibly observed cavitation downstream of the test section probably contributed to the viscosity degradation. In most tests, cavitation was largely inhibited by a circuit supercharge pressure of 100 psi. However, this limited supercharge was not sufficient to suppress all cavitation under a high velocity, high temperature flow combination.

In addition to the limited monitoring of viscosity with the low shear Brookfield apparatus, additional high shear rheometer studies (described later) were later run on stored samples of the fluids. Samples of 0.10, 0.75, and 1.00 per cent solutions were withdrawn from the pipe test facility following the full sequence of pipe tests. Through oversight, similar samples were not available for the 0.25 and 0.50 solutions, so the rheometer tests on these fluids were run on shelf-stored samples of original laboratory mixes which had not previously been exposed to high shear rates.

It is noteworthy that the shelf-stored 0.25 and 0.50 per cent samples were also Brookfield tested before rheometer testing and showed a viscosity reduction of about 50 per cent as compared to the fresh sample viscosities shown in Fig. 3. These samples had been stored about six months and gave no visual or odor evidence of change.

In retrospect, it appears that the viscosity monitoring of these fluids for purposes of detecting degradation was inadequate to give a clear concept of degradation influences. These time and shear degradation influences are further complicated by the fact that, despite random 50 per cent changes in the Brookfield viscosity of the test fluids, rheometer viscosity data per Fig. 9 appear quite orderly. Although this does not obviate the need for better viscosity monitoring of friction tests, it indicates that polymer degradation may not affect high shear friction to the same extent that it affects low shear friction.

III. SHEAR CHARACTERIZATION OF DILUTE SOLUTIONS

A. Characterization at Low Shear Rates

The determination of the shear or viscosity characteristics of a dilute solution of a long-chain polymer is sensitive not only to the concentration, temperature, and rate of shear, but also to the previous history of agitation. This is particularly true as the concentration increases, and thus requires standardization of procedures if reasonably reproducible results are to be obtained.

The standardized method of characterizing laboratory viscosity values for CMC solutions, as recommended by the Hercules Powder Co., is with the Brookfield Synchro-Electric Viscosimeter as made by the Brookfield Engineering Laboratories, Stoughton, Massachusetts. With this convenient instrument, the measurement is accomplished by rotating a small metal spindle in a small sample of the fluid. The spindle is driven by an electric motor via a calibrated torque spring. The value of the driving torque as read from the dial of the instrument may be converted to an equivalent centipoise viscosity reading. The instrument can be calibrated to yield absolute viscosity values with Newtonian fluids, but becomes increasingly relative in nature as the non-Newtonian characteristics of the fluid increase. This instrument was therefore limited to checking the quality of original mixtures and to evaluating degradation of these mixtures under conditions of low rates of shear.

Figure 3 gives averaged values obtained by using the Brookfield instrument to establish the concentration-viscosity characteristics at various temperatures for the concentration range employed in these studies. The samples used in these tests were relatively fresh (2 hours to 20 days) and had been subjected only to the limited shearing of the initial mixing. The data are considered to be essentially free of age, biological, or shear degradation effects. It should be noted that the curves were quite reproducible for concentrations below 0.5 per cent but considerable scatter occurred in data with concentrations greater than 0.5 per cent. The Brookfield No. 1 spindle was used at 60 rpm to measure the lower viscosities. This was progressively shifted to the No. 3 spindle at 12 rpm as the viscosity increased. Some deviation was undoubtedly contributed by this necessary shift in spindle and speed.

Because of the relative lack of turbulent flow data and because of an adequate coverage of laminar flow data relating to CMC solutions, the tests described cover mainly the transition and turbulent flow phases. The data shown in Fig. 3 are, therefore, the only low shear data taken in this program.

B. Characterization at High Shear Rates

The existing studies relative to fluids similar to the non-Newtonian CMC solutions have been thoroughly reviewed and correlated by Metzner and others [3, 10] to yield a workable boundary shear theory. This theory replaces the classical Newtonian laminar pipe flow relation:

$$\tau = \mu \frac{du}{dr} \tag{1}$$

The nomenclature for this equation and those which follow is given on page vi.

The comparable non-Newtonian fluid relation is frequently referred to as the power law and is expressed as:

$$\tau = K\left(\frac{du}{dr}\right)^n \tag{2}$$

While this relation does not universally correlate the shearing characteristics of non-Newtonian fluid flow, it nevertheless contributes to excellent correlation of shear values in the laminar state. It is the simplest and most workable form of relation that has been evolved which does not involve more than two fluid characterizing parameters. With modification and extension this power law also proves a powerful tool in correlating and manipulating shear flow data in the turbulent and transition regions. It is generally accepted that a more universally applicable expression will someday be evolved but will in all probability involve more than two fluid characterizing parameters. For the time being, the power law expression remains the most useful available relation. In consequence of this, one of the prime objectives of the current study was the determination of procedures for evaluating K and n for dilute CMC solutions which might find use in naval applications.

While the values of K and n for a specific fluid and shear condition are not readily measured directly, a fairly simple approach to the evaluation is obtained by making wall shear force measurements for laminar flow in a round tube, using the expression

$$\frac{D\Delta P}{4L} = K'\left(\frac{8V}{D}\right)^{n'} \tag{3}$$

This expression is similar in form to Eq. (2), but fluids obeying the power law involve the relations

$$n' = n$$

$$K' = K\left(\frac{3n+1}{4n}\right)^{n}$$

For the special case of a Newtonian flow, n' has a value of unity, $K' = \mu$, and Eq. (3) is in essence the equation of Poiseuille for laminar pipe flow. For this case the quantity $D\Delta P/4L$ is the wall shear force value and the quantity $8V/D$ is the shear rate at the wall.

In the case of non-Newtonian pipe flow, K' is not equal to μ but serves as an index of consistency; n' on the other hand is an index of the non-Newtonian character. For the pseudoplastic or shear-thinning dilute CMC water solutions, n' varies from unity toward zero as the additive concentration increases and the fluid consistency thickens. In the case of pipe flow with such fluids the quantity $D\Delta P/4L$ continues to measure the wall shear force, but $8V/D$ no longer evaluates the wall shear rate. This is instead given by the expression [10]:

$$\left(\frac{du}{dr}\right)_w = \frac{3n'+1}{4n'} \; \frac{8V}{D} \tag{4}$$

The values of K' and n' are therefore determined by experimental laminar pipe flow tests yielding concurrent measurements of $D\Delta P/4L$ and $8V/D$. From a log-log plot of these data, K' and n' may be graphically determined as intercept and slope values. These values may then be used in the above expression for determining the true value of the wall shear rate or the value of the modified Reynolds number, N'_{Re}, (which will be employed later).

It should be noted [4] that many rheologists prefer to use rotation type rheometers rather than capillary tubes. The capillary tube was, however, considered more appropriate to and sufficiently accurate for the needs of this program.

Numerous forms of Reynolds number have been evolved to provide a correlating fit with various non-Newtonian laminar and turbulent shear data. The form which appears to be most useful in the case of the CMC solutions has been evolved by Metzner and his associates and may be expressed from [10] as

$$N'_{Re} = DV\rho/[K'(8V/D)^{n'-1}] \tag{5}$$

It is important to note that the power law expression may be used for pipe shear flow evaluation in transition flow and turbulent flow as well as in laminar flow. However, the K' and n' values employed in evaluating du/dr and N'_{Re} for flows other than laminar must be determined from laminar flow measurements conducted with an equivalent $8V/D$ value. This means that the principal pipe flow tests in this program, conducted in a pipe of 0.902-in. diameter in order to permit turbulent pressure gradient and velocity distribution measurements, could not be directly used to evaluate the fluid K' and n' values of the test fluids. Instead, supplementary laminar pipe flow tests (or other types of tests) must be employed and these supplementary tests must be conducted for $8V/D$ conditions comparable to those used with the principal test pipe. Since the test pipe facility had been designed to achieve velocities of up to 100 fps, the maximum value of $8V/D$ was expected to be of the order of 1×10^4. Preliminary studies indicated that a laminar flow of this $8V/D$ value could probably be obtained for most of the selected solutions, using an available copper capillary tube of 0.05-in. diameter with the available 100-psi laboratory air supply for driving pressure. It appeared also that this same tube could be operated under measurable laminar flow conditions with ordinary water, thus permitting a fundamental calibration.

This design approach, which follows the recommendations of Bowen [11], results in a simple and inexpensive extrusion type rheometer which is similar in principle to the Ostwald viscosimeter but employing an adjustable pressurized drive in place of gravity. The current design differs from Bowen's in that calibration with water can obviate the need for direct measurement of the tube bore, and adoption of a length of approximately 1000 diameters can eliminate the need for consideration of end effects. Discharge from the rheometer was collected and measured in a graduate and timed with a stop watch. Both the test time and volume discharge were made sufficiently great to allow measurements with an error of no more than about 1 per cent. Where pertinent, the gas-driving pressures were corrected for gravity head contributions.

This rheometer, which was developed late in the program, was operated under controlled temperature conditions to produce the $D\Delta P/4L$ versus $8V/D$ data which are shown in Table I and the dashed curves shown in Figs. 4 - 9. With the exception of the 0.50 and 0.25 concentrations, the fluid samples were those which had been stored following earlier high shear tests in the large pipe facility. The following general observations relate to these figures:

(1) With the exception of the 1.0 per cent solution at 100 F, it appears that all data may be reasonably represented by a suitable straight line in the $8V/D$ range required for analysis of the larger test pipe data ($8V/D = 500$ to 30,000). Because of this, a single graphical determination of the values of K' and n' is presumed applicable over this full $8V/D$ range.

(2) Several of the solutions show some tendency for the data at the extreme left to fall below the selected straight line. This is in accord with the general trends of Fig. 2 and the lower shear rate CMC tests described in [2, 6, 7].

(3) The data for solutions of 0.00 and 0.10 concentration show a tendency to depart from the selected straight line at the right hand end. Calculation and plotting of the critical modified Reynolds number, $N'_{Re} = 2100$, indicate that these departures are simply the beginning of the normal laminar-turbulent transition. Since test data for a given fluid in laminar flow should fit the same line for all pipe sizes when correlated by $8V/D$ as in this plot, the straight line could be expected to extend further to the

right if the selected rheometer bore diameter had been somewhat smaller. Had the rheometer bore diameter been somewhat larger, the given 8V/D data would have encompassed the transition and early turbulent regimes of flow. The straight line of the plot is believed, however, to be adequate for evaluation of the K' and n' pertinent to the desired 8V/D range of 500 to 30,000. More general studies [5] indicate that a natural departure may be expected at some higher 8V/D value.

(4) The data for the 1.0 per cent solution at 100 F appear to depart slightly from a straight line. Because of this, graphical calculation of K' and n' for this curve is local in character and pertains to a tangent to the data curve at a local value of 8V/D.

In accord with these graphical procedures the curves of Figs. 4 - 8 were analyzed to yield the appropriate K' and n' values which are summarized in Figs. 10 and 11.

A study of these K', n' data supports the following general observations.

(1) The n' or slope values progress in an orderly manner from the maximum value of unity to a minimum of about 0.4.

(2) Even modest temperature changes have a substantial influence on n' and a very large influence on K'. The influence on K' is roughly in accord with the Brookfield viscosity data shown in Fig. 3, and is also roughly in accord with standard temperature-viscosity variations for plain water.

(3) Uncontrolled degradation effects probably are contained in the data and possibly have had some influence on the indicated n' values and substantial influence on the indicated K' values. Degradation probably tends to reduce K' and increase n'. The data of Fig. 9 are, therefore, conservative for any design applications.

(4) It is to be noted that the K' value from tests of the

0.00 per cent solution (plain water) at 70 F is approximately 5 per cent higher than a standard value of μ for water. This standard value could be used to revise the value of the tube diameter to achieve a fit or calibration with the standard K'. However, since the revision of diameter would be modest, the nominal tube diameter of 0.05 in. was employed throughout the calculations.

IV. FLOW STUDIES IN A CIRCULAR SMOOTH PIPE

A. The Test Facility

1. The Test Section

The diameter and length of the cylindrical test section were selected to permit a mean velocity ranging up to 100 fps with a wide range of fluids. The pumping unit available for recirculating service was a 25 hp centrifugal type whose head-discharge characteristics were estimated to be suitable for the resistances which might be imposed by a test section of about 1-in. diameter and 100 diameters in length.

The literature relating to the length requirements for flow establishment in a pipe with non-Newtonian fluids appears to be fragmentary and inconclusive. Published values for the length of flow establishment range from 30 diameters to several times this number. In view of this, a length of 100 diameters was arbitrarily selected. This was deemed adequate for most tests yet not excessive in terms of the available pumping power.

The inside diameter of the test section was finally established as 0.902 inches. This resulted from selecting a standard, welded, Type 304, stainless steel, sanitary tubing of 1.000-in. outside diameter and 0.049-in. wall (Trent Tube Co.). Since the welded type tube is formed from sheets of uniform thickness, the inside diameter can be accurately determined by micrometer measurements of outside diameter, inside diameter, and wall thickness at the tube ends and with outside diameter measurements along the tube length. These measurements established that the inside diameter varied less than a few thousandths of an inch in measurements along the length or in measurements of roundness.

The interior of the tube was factory ground by an abrasive belt impregnated with a No. 180 grit. This was the smoothest production finish available at the time of procurement. The surface roughness was not mechanically measured, but subsequent tests with water established that the surface was "hydraulically smooth". The pipe itself was carefully aligned.

Flow into the 0.902-in. diameter test section was from a concentric 12-in. diameter approach pipe capped with a flat plate normal to the flow axis. The transition curve from the flat plate to the cylindrical test section was the quadrant of an ellipse conservatively selected in accord with the findings of Ref. [12]. The equation in this case was $(x/1.353)^2 + (y/0.226)^2 = 1$ in inch values. The transition was an accurately machined and polished metal piece fitted flush with the surface of the large cap plate at the upstream end and flush with the test section wall.

The first pair of boundary wall pressure measuring taps was placed 0.90 in. ($\approx$ 1 diameter) downstream of the junction of the entrance transition and the test section. These were designated as tap No. 1 and were arbitrarily considered to constitute the origin of boundary layer growth. Ten additional pairs of pressure measuring taps designated as Nos. 2 through 11 were placed at 9.00-in. centers ($\approx$ 10 diameters) along the test section for a total measuring length of 100 diameters. In order to minimize curvilinear flow contributions from the downstream expansion following the test section, the test section cylinder was extended 10 additional diameters beyond the last pair of pressure taps before beginning the flow expansion.

To minimize the possibility of bad tap geometry, secondary flows, and excessive resistance through the 1/32-in. diameter pressure tap holes, all taps were arranged in pairs which were diametrically opposed across the test section. Subsequent check tests showed that both holes of a pair consistently agreed with each other to within a fraction of a per cent of the mean velocity dynamic head.

Because of the very high velocities (up to 100 fps) contemplated for the test program, it was deemed essential to provide pressure taps of high quality. The most pertinent investigations [13, 14] on pressure taps appeared to support the use of sharp-edged, burr-free holes of about 1/32-in. diameter. Such holes should permit measurements with an error of no more than 0.25 per cent of the dynamic head. Since the usual procedure of drilling and honing the tube wall to obtain sharp, burr-free holes involves difficulties in machining and inspecting in small bore tubes of long length, a new procedure was tried in this assembly. This procedure involved burning the hole rather than machining it, and utilized an "Elox" burning machine. The electrically burned hole is just a few thousandths of an inch larger than the burning electrode and leaves a hole of uniform quality without any apparent rounding or burring of the edges. As mentioned previously, pressure checks between opposed members of paired holes were consistently in good agreement.

Expansion of the 0.902-in. diameter of the test section to the 4-in. diameter pipe leading to the recirculating pump was accomplished with a boundary transition curve which was tangent to the test section exit wall and tangent to the entrance wall of a conical diffuser of 5 degrees total interior angle. The transition curve had a length of approximately 2 test section diameters and was a parabola with equation $y = 0.012101x^2$ in inch values. The transition and low angle cone were selected to minimize separation eddies and the consequent cavitation which was likely to occur with the very high exit velocities and low pressures normal to this part of the flow circuit. However, despite the conservative selection of boundary geometry, the low exit pressures created by the high frictional losses of the test section required supercharging of the tunnel circuit to suppress cavitation in the transition region. For many of the high velocity tests, a supercharge pressure of 100 psi gage was required at the 12-in. approach to the test section to achieve cavitation suppression in the downstream transition.

2. The Recirculating System

The prime function of the recirculating system is to provide a return flow conduit between the exit and entrance of the test section. This conduit must contain a pump capable of supplying the energy losses generated in the flow loop and must supply a low-turbulence, quality flow to the test section.

In this case the pumping energy was supplied initially by a 25 hp centrifugal pump with a nominal rating of H = 105 ft, Q = 700 gpm. With simple valve throttling this pump served to provide selection and stable control of test section velocities in the range from 10 to 100 fps. However, the relatively large energy input of this pump was excessive for most of the low speed runs and contributed to difficulties in temperature control. Consequently, in the later runs a smaller by-pass pump was used for a velocity range from about 4 to 35 fps, and this materially improved the temperature control. The smaller pump was a 3 hp unit with a nominal rating of H = 47 ft, Q = 50 gpm.

Cavitation difficulties were encountered in the pump suction as well as in the test section diffuser. For low and intermediate velocities, a supercharge pressure of 40 psi gage at the test section entrance was found necessary for suppression of cavitation. For the higher velocities, a supercharge of up to 100 psi was used.

In order to reduce vibration in the flow circuit, the pumps were connected to the circuit piping by rubber hoses. This was not completely successful and some vibration did exist in the test section during the tests.

The circuit piping primarily comprised standard 125-psi piping and fittings of 4-in. and 12-in. size. The 12-in. size was employed to provide a low velocity, low turbulence approach to the horizontal test section.

The 12-in. lower leg of the tunnel was fitted with three copper heat exchanger coils through which ice water was circulated for control of test fluid temperature. The system provided effective control in the range from 70 to 100 F.

In order to minimize metallic contamination of the test fluid, all interior surfaces of the flow circuit were epoxy coated, with the exception of the stainless steel test section, the copper heat exchanger tubes and the bronze valve and pump members. The ferric parts of the pump case and valve housings were metallized with zinc.

3. Pressure Measurements

All of the primary test data, including the pipe friction gradients, flow discharge, and velocity profiling, were interpreted from pressure values measured with simple U tube manometers connected to appropriate pressure measuring taps. These manometers employed reading lengths up to 14 ft and gage fluids ranging in specific gravity from 1.20 to 13.6. Lengths and specific gravities were selected to match the conditions of a particular test to permit readout with errors of no more than 1 per cent of the dynamic pressure.

4. Temperature Measurements

Fluid test temperatures were measured with a precision glass tube thermometer (graduations 0.1 F) inserted in a water-filled metal well which projected 3 in. into the top of the 12-in. approach pipe to the test section.

5. Discharge Measurements

A measure of the test section flow discharge was essential for evaluation of the mean flow velocity. For these tests the discharge was measured by a calibrated constriction type flow meter. The flow metering involved the measurement of the pressure head drop, H, which occurred where the flow passed from the 12-in. approach pipe to the 0.902-in. test section through the entrance transition. This elliptical boundary curve was previously discussed in the test section description and bears some resemblance to a standard flow nozzle.

The upstream pressure measurement was made in the stagnation corner formed by the 12-in. pipe wall and the cap plate. The downstream pressure measurement was made at test section boundary tap No. 1.

The relation between the pressure differential and the discharge was established by temporarily breaching the tunnel loop to provide a non-recirculating flow by using the laboratory water supply. With this setup the discharge from the test section could be collected in a volumetric measuring tank for a range of flow values. The resulting water calibration curve is shown in Fig. 12. While it would have been desirable to obtain similar calibration curves with the actual non-Newtonian fluids, the cost of assembling a breached recirculating system together with a large supply of the fluid appeared unwarranted in the initial phases of this project. In consequence, the calibration curve of Fig. 12 was used for all tests with the assumption that for a given pressure difference across the nozzle, the velocity was essentially the same whether water or a non-Newtonian fluid was used. Some error is undoubtedly involved in this assumption but additional tests will be required to establish the relation between the discharge coefficient, C_D, and the modified Reynolds number N'_{Re}. Because of the large contraction ratio and near-potential flow conditions, the error is believed small.

6. Velocity Profile Measurements

Velocity profiles were measured in the plane of the No. 10 boundary wall pressure measuring taps by traversing a Pitot type of total head tube across a vertical diameter of the pipe. The Pitot consisted of a square cut stainless steel sting of 0.042-in. outside diameter, 0.025-in. inside diameter, and 0.62-in. length. This sting was placed in axial alignment in the pipe and supported by a strut whose cross section was approximately 1/8 in. long in the flow direction and 1/16 in. in width normal to the flow. The upstream and downstream edges were semi-circular in form. The sting could be traversed from wall to wall by an external screw arrangement monitored with a dial micrometer. With calibration, the sting position could be determined to within a few thousandths of an inch. Velocity values were inferred from a differential manometer with one leg connected to the Pitot sting and the other connected to the No. 10 pair of wall pressure taps.

B. The Flow Studies

1. Hydraulic Gradient and Length of Flow Establishment

As indicated in the discussion pertaining to the selection of test section length the literature relating to the length requirements for flow establishment in a smooth pipe with non-Newtonian fluids appears to be inconclusive. In this study, therefore, boundary pressure measuring taps were placed at 10-diameter intervals along the axis of the test section for the first 100 diameters following entrance. The pressure differences between successive pairs of these taps were read out with manometers for a series of tests in which the additive concentration and mean velocity were progressively varied. The resulting data for 70 F conditions are tabulated in Table II and are plotted as dimensionless hydraulic gradients (head loss $\Delta H/\frac{V^2}{2g}$ versus distance from entrance X/D) in Figs. 13 through 17. The listed values of N'_{Re} were calculated for conditions in the vicinity of $X/D = 90$.

The prime objective of these tests was to determine whether data from the downstream pressure taps could be construed as representing fully developed flow. A study of these dimensionless plots indicates that for all practical purposes frictional measurements between the pairs of taps which are ninety and one hundred diameters downstream (Nos. 9 and 10) represent a condition of established flow. It is recognized that establishment of a uniform boundary pressure gradient is not an absolute or highly sensitive measure of complete flow establishment but is generally accepted as a fair measure of the end of major changes relating to frictional values. In consequence, the frictional data of this study are mainly taken from the pressure drop measurements between taps Nos. 9 and 10. In a few instances of low pressure differentials between 9 and 10, where the gradient appeared flat over a greater distance, a greater ΔL distance was used to provide more accurately readable ΔP values. In those instances where greater ΔL values were used, the pertinent pressure tap increment is indicated in the listings of Table No. III.

It may be noted from a study of Figs. 13 through 17 that in most cases the gradient represents a smoothly diminishing slope with increasing distance from the pipe entrance. One might speculate that this smooth progression would be normal for a near laminar flow and might also be evident in a turbulent flow where the transition from laminar occurred very close to the entrance. However, in a few instances (most notably Run No. 54 of Fig. 14) the lower concentrations show evidence of an inflexion in the gradient, which is indicative of the laminar-turbulent transition occurring well beyond the pipe entrance. The influence of turbulence ($N'_{Re} > 2100$) on head loss is markedly evidenced in these figures.

From the hydraulic gradient data the length of smooth pipe flow establishment appears to vary between about 20 and 80 diameters, depending on flow conditions.

2. Laminar, Transition, and Turbulent Studies in Established Test Pipe Flow

Upon completion of the studies which determined that established flow existed at the Nos. 9 and 10 pressure taps, these taps were subjected to a test program for the evaluation of the local pipe friction. This consisted of concurrent measurements of the mean velocity V and the ΔP over a distance of 10 diameters. These tests were conducted with the velocity ranging from about 5 to 100 fps, temperature ranging from 70 to 100 F, and the CMC solution concentration ranging from 0 to 1.0 per cent. The resulting data were then calculated and plotted as $D\Delta P/4L$ versus $8V/D$ values in Figs. 4 through 8. This was handled in the same manner as previously described for the small tube rheometer data. The curves from Figs. 4 through 8 were then combined to form the composite treatment of Fig. 9 for an improved perspective of the total coverage.

The following observations relate to these data:

1. Although the pipe tests with 0.00 concentration (plain water) were not extended into the transition or laminar flow regimes, there is every reason to believe that diminishing test values of $8V/D$ would define a conventional

transition regime and an eventual junction with the rheometer curve near the critical $N'_{Re} = 2100$.

2. An arbitrary laminar to turbulent critical transition value of $N'_{Re} = 2100$ for the pipe is shown with the rheometer data of Fig. 9. Analysis by others [15] indicates that this approximates a lower limit value and may on occasion rise to substantially higher values. With the exception of the laminar pipe test data for the 0.75 per cent solution, the value of $N'_{Re} = 2100$ appears to serve as an approximate limit to the laminar range of the pipe test data.

3. The apparent failure of the laminar pipe test data and the laminar rheometer data to fall on a common line in the summaries of Fig. 9 are believed due to a combination of degradation effects and the ignoring of the fall-off in shear at the left end of the rheometer data, as previously discussed.

4. Transition flow with the more dilute solutions (0.10 per cent per Fig. 4) covers a very substantial range of shear forces and a steep rate of change. This was also accompanied by instabilities in the manometer ΔP values involving a wide range of shear values. In contrast to this, with increasingly concentrated solutions the transitions cover a progressively smaller range of shear values and the transition occurs without evidence of instability. This could indicate real stability but might be partially due to the excessive damping which occurs in the manometer read-out system. Others [2] have observed, however, that the scale of turbulence appears to increase with the heavy concentrations and to result in a slower, more gentle "kneading" action.

5. With the heavy 1.00 per cent solution at 70 and 85 F, transition to full turbulence is not evident within the available range of shear rate. For these fluids, much of the transition data appears to be nearly linear. (It is noteworthy that limited data by Dodge and Metzner [15] also

show this lack of a definite swing to turbulence.) In contrast, data for the same concentration at 100 F seem to distinctly break and to approximate the turbulent data for lesser concentrations.

6. Figure 9 indicates that at high rates of shear all of the test fluids except the 1.00 per cent solution show a fully developed turbulent branch of a linear nature similar to the turbulent branch of Newtonian fluids. The slope of the turbulent data line appears to diminish as the non-Newtonian index, n', decreases. It seems probable that all turbulent data may ultimately become non-linear at some higher rate of shear not evidenced within the limits of these tests.

7. The general pattern of Fig. 9 would indicate that the major frictional reductions which occur with dilute solutions of CMC do not result from delaying the onset of turbulence. It appears instead that the benefits largely result from some mechanism of the turbulence, a mechanism which is less consumptive of energy by reason of the presence of the additive. This reasoning does not, however, apply as readily to the data of the 1.00 per cent solution where friction benefits are largely due to delayed turbulence.

8. Temperature appears to have a relatively small effect on wall shear forces in the turbulent regime of flow. This is in marked contrast to the laminar regime in which modest temperature changes produced substantial shear changes.

9. The influence of pipe size, as evidenced by comparing the rheometer and test pipe data of Fig. 9, indicates that for a given fluid all laminar flow data will tend to fall on a common line. In contrast turbulent flow data organize on this $D\Delta P/4L$ versus $8V/D$ plot only for a unique pipe size. Lack of fully developed turbulent flow data for the rheometer prevents further correlation of this size effect, but Bowen [16] provides a procedure for such a correlation.

10. The influence of the additive on wall shear force values is remarkably great for the high shear rate, turbulent flow conditions.

The foregoing presentation and discussion of the shear data in the form of $D\Delta P/4L$ versus $8V/D$ provide a most useful form of flow characterization for many purposes. However, a very substantial amount of the more general studies of flow friction have resulted in data presentations in the form of f versus N_{Re}. In order that the reader may use this more familiar form of presentation, the basic data for Fig. 9 have been alternately calculated to provide the f versus N'_{Re} presentation of Fig. 18.

It should be noted that in Fig. 18 the frictional value, f, is the Fanning f as commonly used by the rheologist, rather than the Darcy f as commonly used by the engineer. The Darcy f is four times as large as the Fanning f. It should also be noted that the abscissa values are in terms of the modified Reynolds number, N'_{Re}, previously given by Eq. (5) which permits a reasonable correlation of both Newtonian and non-Newtonian fluid data.

As a framing reference it may be noted that flow which is essentially laminar corresponds to the theoretical laminar curve $f = 16/N'_{Re}$ and evidences of the beginning of transition occur in the vicinity of $N'_{Re} = 2100$. On the other extreme, fully turbulent flow data for plain water (0.00 per cent concentration) show good conformance with the Karman-Prandtl smooth pipe curve.

Dodge and Metzner [15] found that data for a wide variety of non-Newtonian slurries and polymers correlated in a generalized way when plotted in the manner shown in Fig. 18. The correlation consisted of a family of curves differing in n' and with the curve equations being an empirical modification of the Blasius equation. In their correlation, the f varied with the concentration as expressed through the n' value but proved independent of pipe size. However, in limited tests with a CMC solution they obtained data with much lower f values and with a distinct size dependency as compared to the other fluids. Shaver and Merrill [2] also correlated other data with still another modification of the Blasius equation. However, the equation failed to make a reasonable fit when tried with the data of the current study. As yet, the physical properties which determined these performances are undefined and a general correlation has not been obtained. Whether this peculiar difference will also be found in high shear tests with other polymer solutions remains to be seen.

On the basis of the findings of Dodge and Metzner and in view of the fact that the turbulent data of Fig. 18 represent only one pipe size, the data should not be applied to other sizes.

It is of interest to note that with dilute solutions in the current study the transition from laminar to turbulent shows as an abrupt rising instability consistent with that of water. However, for the 1.00 per cent solution at 70 F there is no evidence of a distinct transition to turbulence. Using a 0.30 per cent solution, Dodge and Metzner found a similar lack of clear transition, but Bowen [16] found a distinct transition with a similar solution.

3. Velocity Profiles for Established Flow

During the course of these studies, attempts were made to obtain turbulent pipe flow velocity profiles, using the Pitot equipment previously described. Initial profiles were run with plain water for validation of technique, and resulted in discharge checks agreeing within 2 per cent. Since the prime interest of this program was the evaluation under distinctly non-Newtonian conditions with fully developed turbulent flow conditions, the first studies were made with 0.50 and 0.75 per cent solutions and with velocities in the 50 to 70 fps range. These tests led to a long series of broken Pitot stings and relatively little data. The data which finally did result did not, however, yield agreement of the flow meter discharge and the integrated Pitot discharge. The lack of agreement was of the order of 5 to 10 per cent and discouraged presentation of the data. An attempt to rationalize the error indicated three possible sources, as follows:

(a) Shortcomings in the Pitot fabrication or peculiarities in the non-Newtonian fluid may have induced vibration of the probe sting.

(b) The metered discharge with flow constriction nozzle coefficients taken from Fig. 12 (Reynolds number based on water) may not be applicable to discharges with the higher concentrations of additive.

(c) Pitot coefficients for the heavy additives may depart substantially from the conventional near-unity values. It has been established by numerous investigators [17] that, with Newtonian fluids, Pitot tubes operating under very low Reynolds number conditions (N_{Re} based on Pitot sting diameter < 500) show rapidly decreasing coefficients with decreasing values of N_{Re}. If the large viscosity values of Fig. 3 are assumed pertinent to the flow around the small Pitot tip, even relatively large velocities will yield the low Reynolds numbers which cause coefficient difficulties.

In view of the difficulties with the heavy concentrations, two additional profiles were run with the 0.10 per cent solution in order to minimize the probable contribution of items (b) and (c). The Pitot sting again broke during the last of these runs, resulting in one final effective profile. This profile, as with plain water, yielded agreement of the flow meter discharge and the integrated Pitot discharge. Program termination necessitated the abandonment of further profiling.

In view of the fact that only one usable profile was obtained and is in itself inadequate for establishing any general pattern of flow, it is not presented at this time.

Despite the foregoing difficulties, it is strongly recommended that future experimental studies attempt to obtain adequate velocity profiles to verify the existing theoretical profiles [10]. Validation of such theories is necessary for establishing correlation with flat plate theories in accord with Granville [18].

Future profile experiments conducted with a larger test pipe diameter and a larger Pitot sting may, in accord with Fig. 9, permit fully turbulent studies without excessively high velocities.

V. CONCLUSIONS

The addition of small quantities of CMC to fresh water produces a greatly thickened fluid possessing non-Newtonian flow properties. As compared to water, this fluid shows a substantial increase in resistance to flow in the laminar regime and greatly decreased resistance to flow in the fully turbulent regime.

The preparation, storage and handling of CMC solutions appear to present no serious problems to eventual naval applications.

The power law relation which is frequently used to characterize non-Newtonian flow processes proves to be an adequate analytical and design tool for engineering studies with CMC solutions. These tests serve to better define the K' coefficient and n' exponent necessary to the evaluation of the power law relation.

For a given dilute solution, the K' and n' values appear to be essentially constant for a wide range of flow conditions pertinent to engineering applications.

The temperature of the solution has a substantial influence on shearing resistance in the laminar flow regime but a relatively small influence in the fully turbulent regime. For all measured concentrations of CMC, the values of K' and n' tend to gradually approach that of water as the temperature increases. The rate of change of K' is much greater than that of n'.

The influence of additive concentration on the index n' is quite marked with small concentrations and relatively less as the concentration increases. The value of n' gradually decreases from unity with concentration increase.

CMC solutions degrade or change in their chemical and flow shear properties as some function of time and exposure to shear. The influence of degradation on shear appears to be greatest with low rates of shear. The shear flow data presented herein relate to degraded fluids. Fresher fluids will presumably offer even greater shear reduction benefits.

Frictional data from these and other tests of CMC solutions fail to correlate uniquely with data from tests of a wide variety of slurries and other long-chain polymer non-Newtonians. CMC reduces the friction even more than other common polymers.

Blow-down capillary rheometers provide a practical and relatively inexpensive method for determining the rheological characteristics of CMC solutions.

VI. RECOMMENDATIONS FOR FUTURE WORK

Other long-chain polymer solutions have shown promise of good frictional reductions under high shear conditions. The shear flow characteristics of these materials should be comparatively evaluated over a wide range of conditions.

Shear flow studies should emphasize determination of n' and K' values over a wide range of shear rates (100 to 100,000 sec^{-1}) and temperatures (35 to 100 F) using one or more sizes of capillary rheometer. The rheometer data should extend into fully developed turbulent flow.

Rheometer evaluations of additives should include both fresh and sea water as solvents.

Larger pipe flow studies should be conducted to permit evaluation of the mode of flow establishment and the velocity profiles for transition and fully developed turbulent flows. If possible, these studies should be carried to the fully laminar regime and should also include determination of a suitable instability parameter as a function of radial position.

All shear flow studies should be carefully monitored for degradation of character of the additive. Monitoring should assure that all flow data represent fresh materials as they would normally be employed in naval applications and the extent to which degradation will influence frictional values in the applied case.

Secondary studies should be conducted to better establish the coefficients of flow meters, Pitots or other shear-sensitive devices employed in the shear flow evaluations of the non-Newtonian fluid.

Secondary tests should be conducted to establish the existence or non-existence of viscoelastic properties in the solutions and of wall slip in the flow. The possibility of wall slip should be checked by the use of more than one size of rheometer, in accord with [5].

LIST OF REFERENCES

[1] Ousterhout, R. S. and Hall, C. B. "Reduction of Friction Loss in Fracturing Operations", Journal of Petroleum Technology, March 1961.

[2] Shaver, R. S. and Merrill, E. W. "Turbulent Flow of Pseudoplastic Polymer Solutions in Straight Cylindrical Tubes", Am. Inst. of Chemical Engineering Journal, Vol. 5, No. 2, June 1959.

[3] Metzner, A. B. "Non-Newtonian Technology", Advances in Chemical Engineering, edited by Drew and Hoopes, Academic Press, New York, 1956.

[4] Fabula, A. G. Note on Torpedo Drag Reduction with a Non-Newtonian Turbulent Boundary Layer, U. S. Naval Ordnance Test Station, Pasadena, Technical Note P508-18, July 1961.

[5] Thomas, D. G. "Significant Aspects of Non-Newtonian Technology", Progress in International Research on Thermodynamic and Transfer Properties, ASME, 1962.

[6] Salt, D. L., Ryan, N. W., and Christiansen, E. B. "The Rheology of Carboxymethylcellulose Dispersions in Water", Journal of Colloid Science, Vol. 6, 1951.

[7] Crawford, H. C. and Pruitt, G. T. Rheology and Drag Reduction of Some Dilute Polymer Solutions, a report by Westco Research, The Western Co. of North America, July 1962.

[8] Anon. Hercules Cellulose Gum-Properties and Use, Hercules Powder Co., Wilmington, Delaware, 1960.

[9] Rodriguez, F. and Winding, C. "Mechanical Degradation of Polyisobutylene Solutions", Industrial and Engineering Chemistry, Vol. 51, No. 10, Oct. 1959.

[10] Metzner, A. B. "Flow of Non-Newtonian Fluids", Handbook of Fluid Dynamics, edited by Streeter, McGraw-Hill Book Co., New York, 1961.

[11] Bowen, R. L. "Best Methods for Obtaining Flow Data", Chemical Engineering, Aug. 21, 1961.

[12] Rouse, H. and Hassan, M. M. "Cavitation Free Inlets and Contractions", Mechanical Engineering, March 1949.

[13] Rayle, R. E. "An Investigation of the Influence of Orifice Geometry on Static Pressure Measurements", MS Thesis, M. I. T., 1949.

[14] Shaw, R. "The Influence of Hole Dimension on Static Pressure Measurements", Jour. of Fluid Mechanics, Vol. 7, Part 4, April 1960.

[15] Dodge, D. W. and Metzner, A. B. "Turbulent Flow of Non-Newtonian Systems", Am. Inst. of Chemical Engineering Journal, Vol. 5, No. 2, June 1959.

[16] Bowen, R. L. "Designing Turbulent Flow Systems", Chemical Engineering, July 24, 1961.

[17] Folsom, R. G. "Review of the Pitot Tube", Trans. ASME, Oct. 1956.

[18] Granville, P. S. "The Frictional Resistance and Boundary Layer of Flat Plates in Non-Newtonian Fluids", David Taylor Model Basin Report No. 1579, Dec. 1962.

F I G U R E S

(1 through 18)

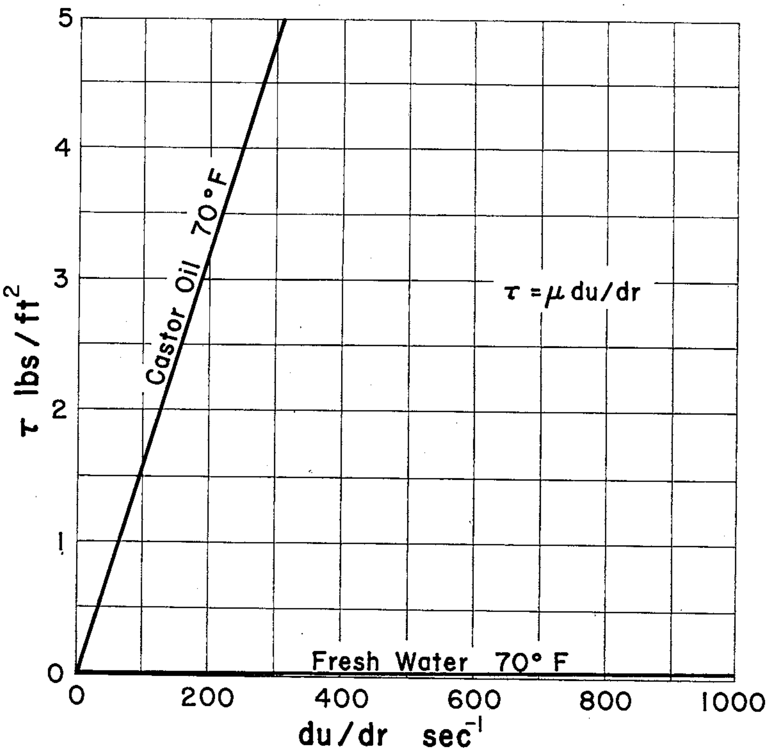

Fig. 1 - Arithmetic Plot of Laminar Fluid Flow Data for Newtonian Fluids

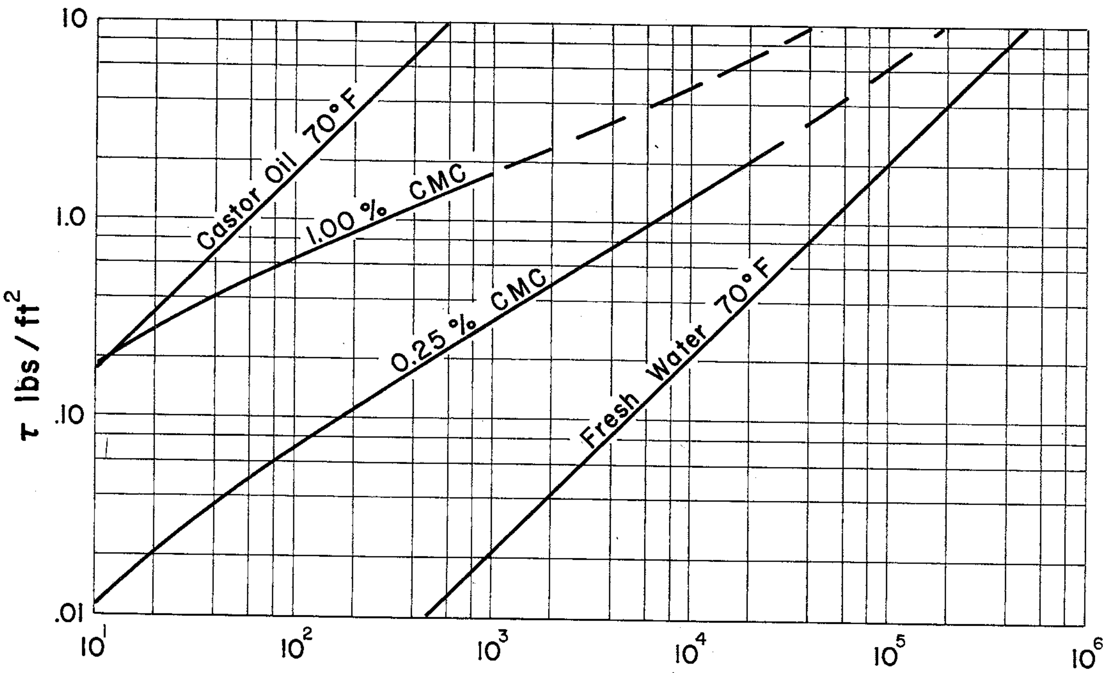

Fig. 2 - Logarithmic Plot of Laminar Fluid Flow Data
for Newtonian and Non-Newtonian Fluids

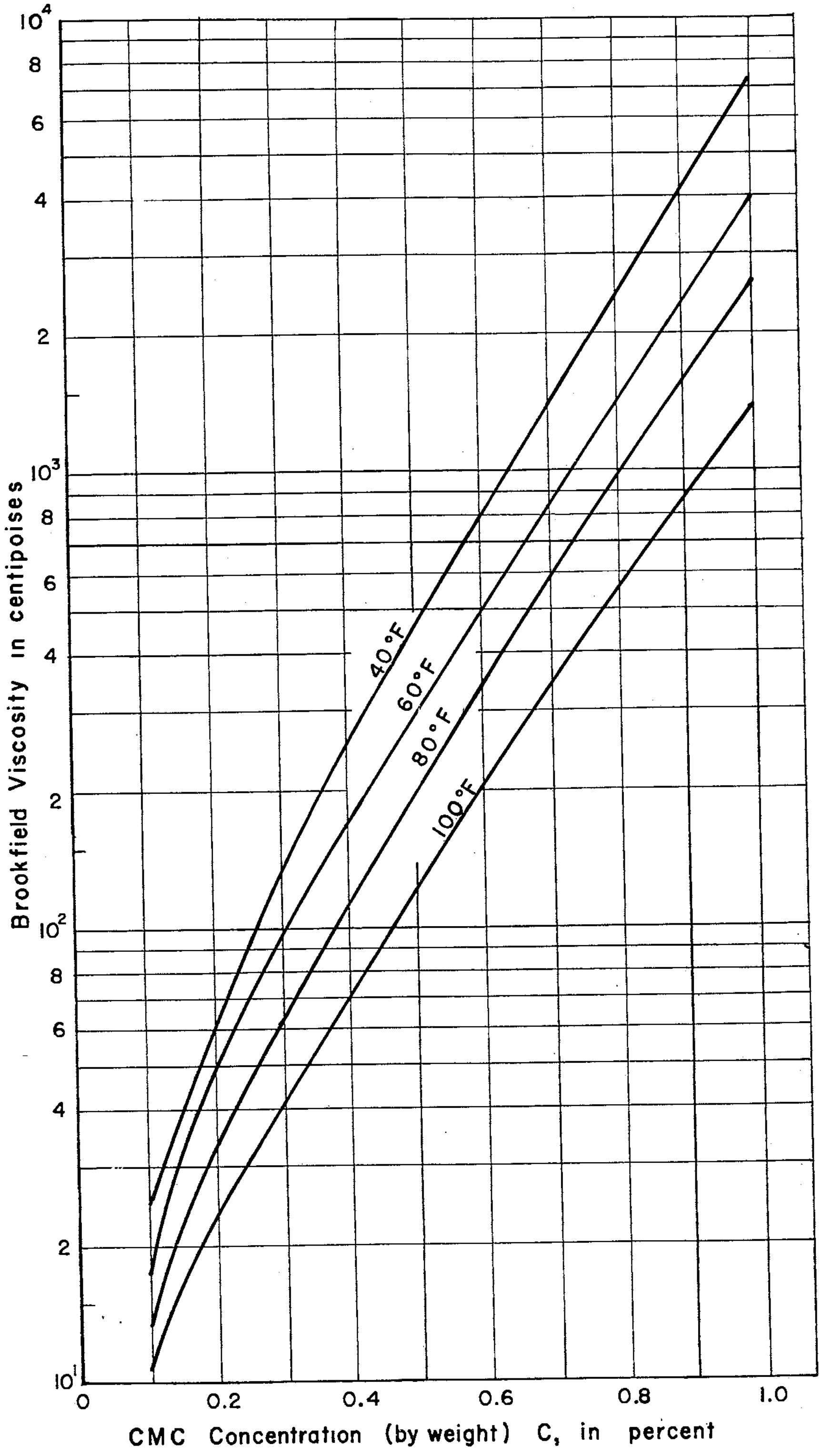

Fig. 3 - Concentration-Viscosity Properties at Various Temperatures for CMC Solutions at Low Shear Rates

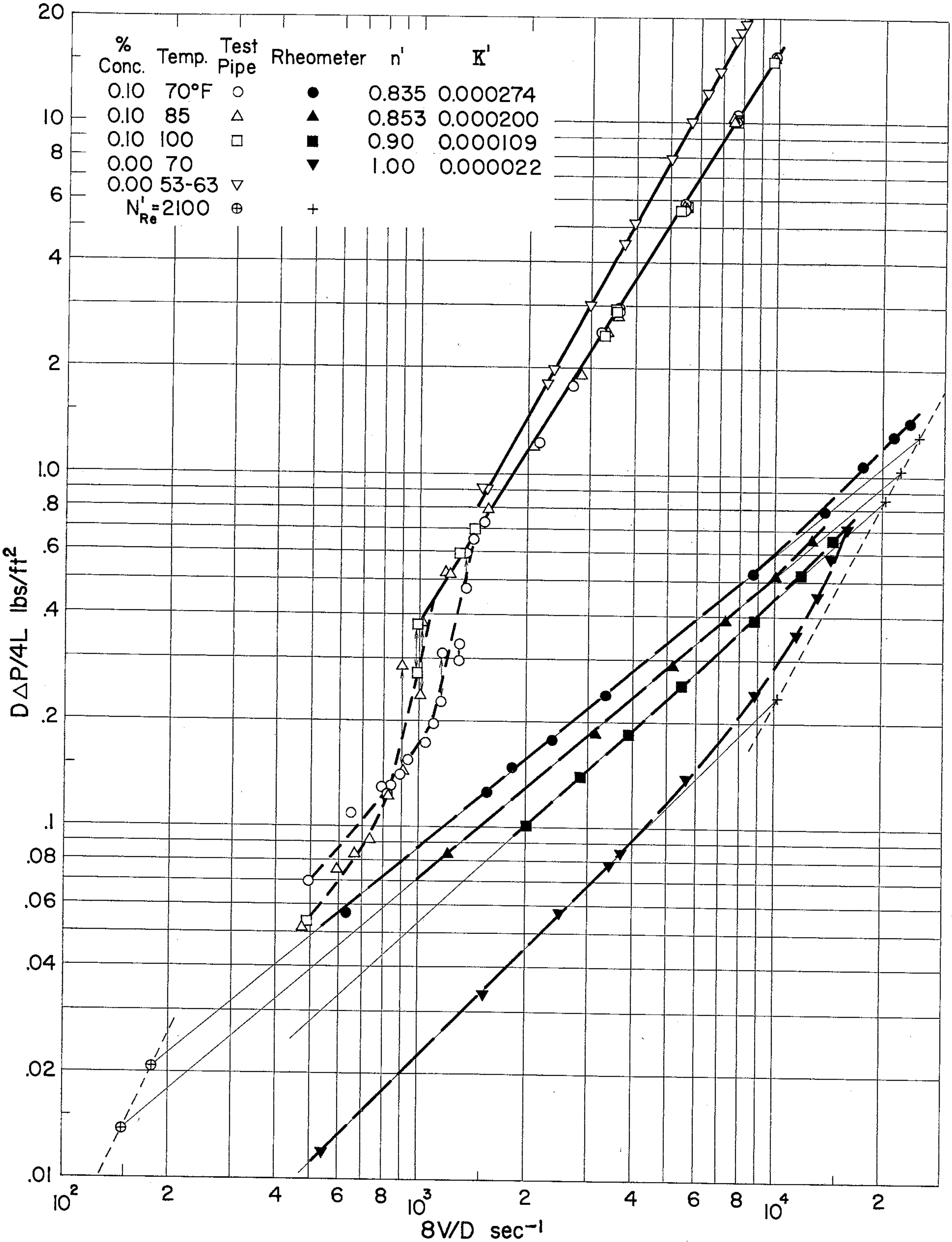

Fig. 4 - High Shear Rate Characterizations for 0.00 and 0.10 per cent CMC Solutions

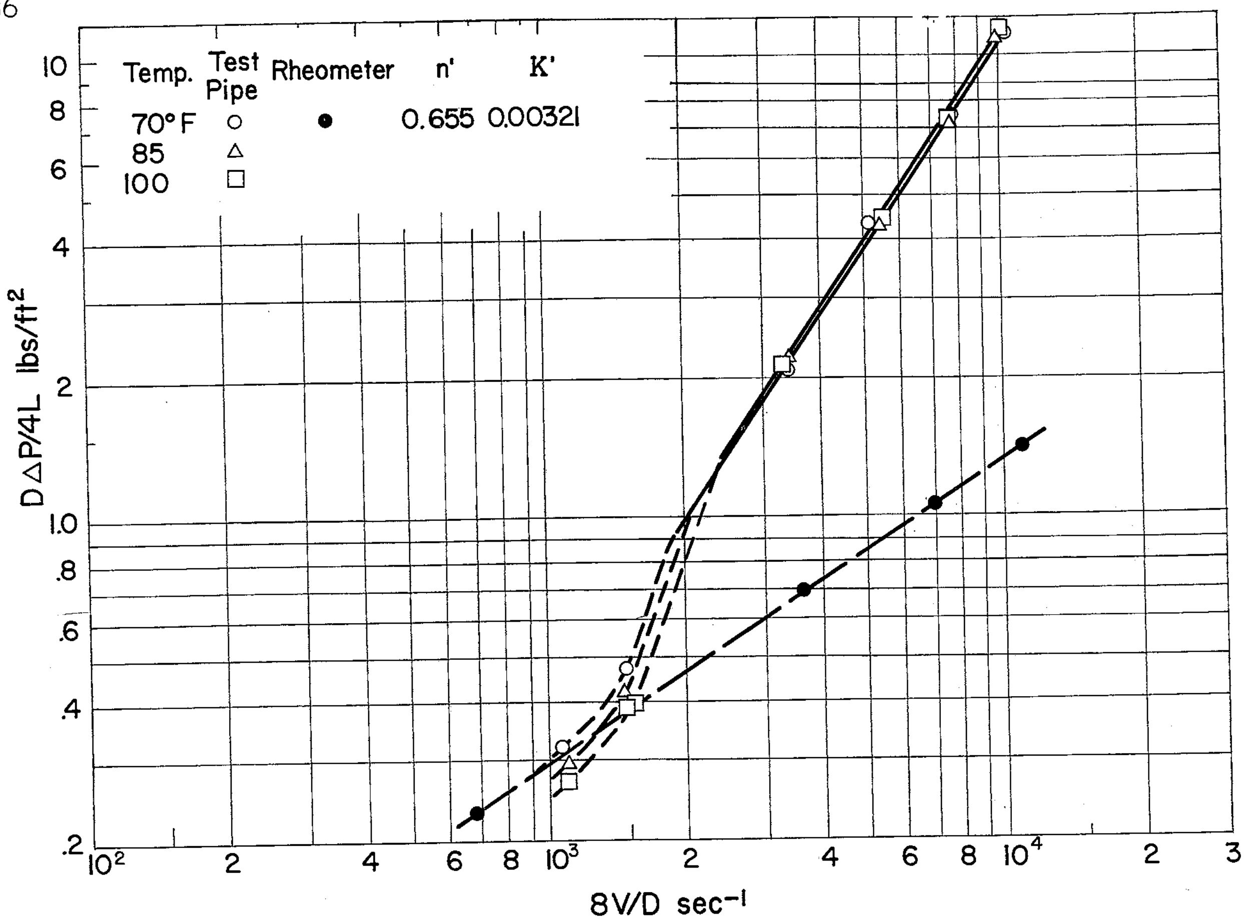

Fig. 5 - High Shear Rate Characterizations for a 0.25 per cent CMC Solution

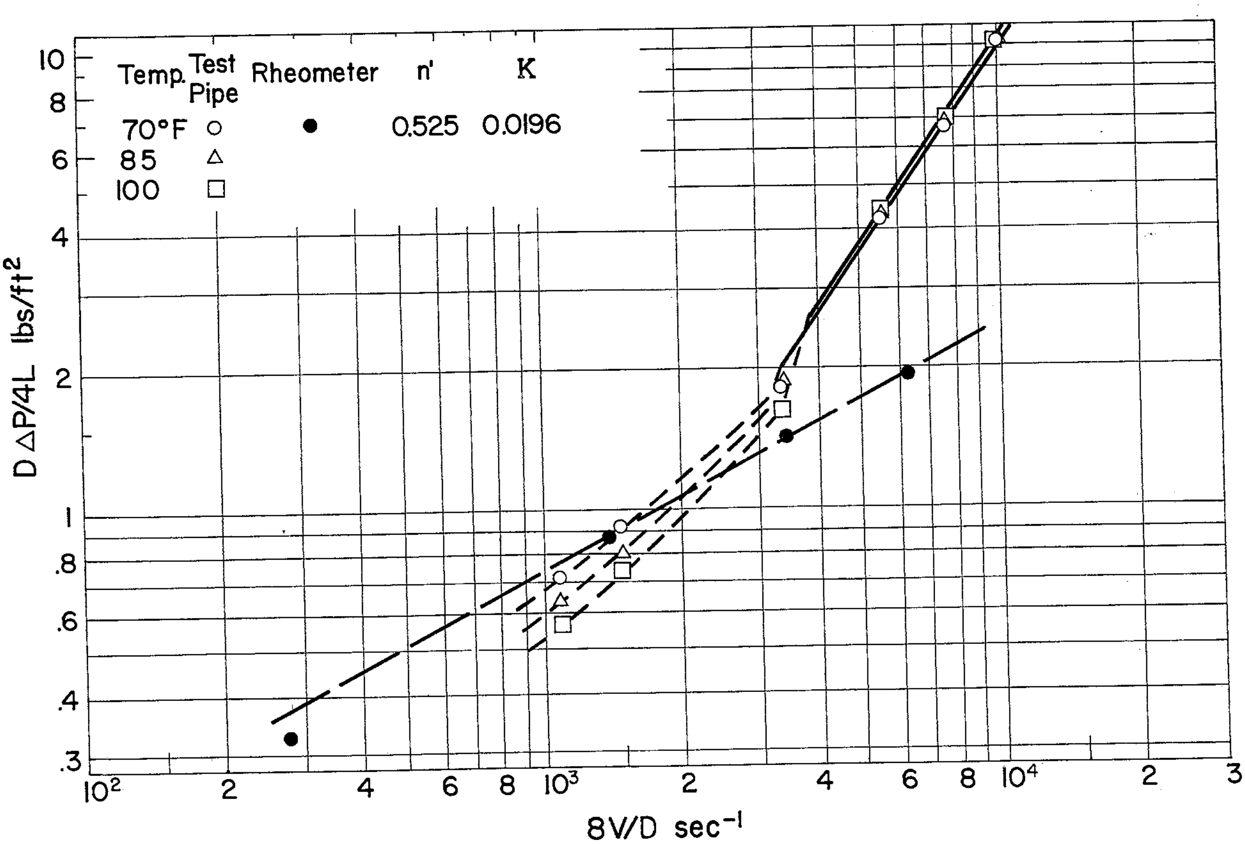

Fig. 6 - High Shear Rate Characterizations for a 0.50 per cent CMC Solution

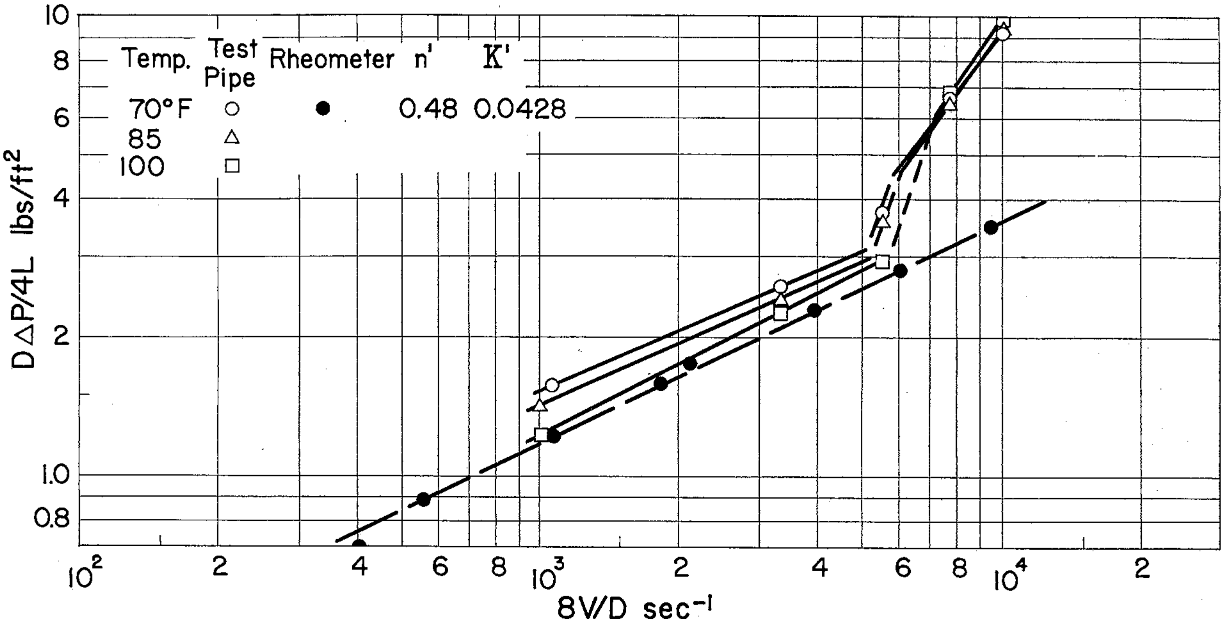

Fig. 7 - High Shear Rate Characterizations for a 0.75 per cent CMC Solution

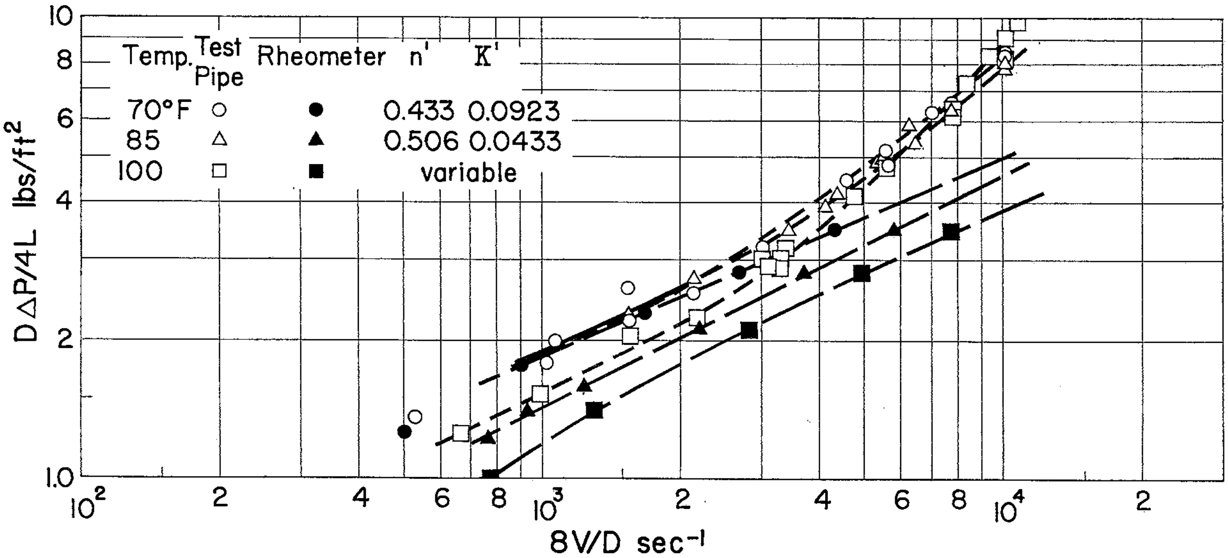

Fig. 8 - High Shear Rate Characterizations for a 1.00 per cent CMC Solution

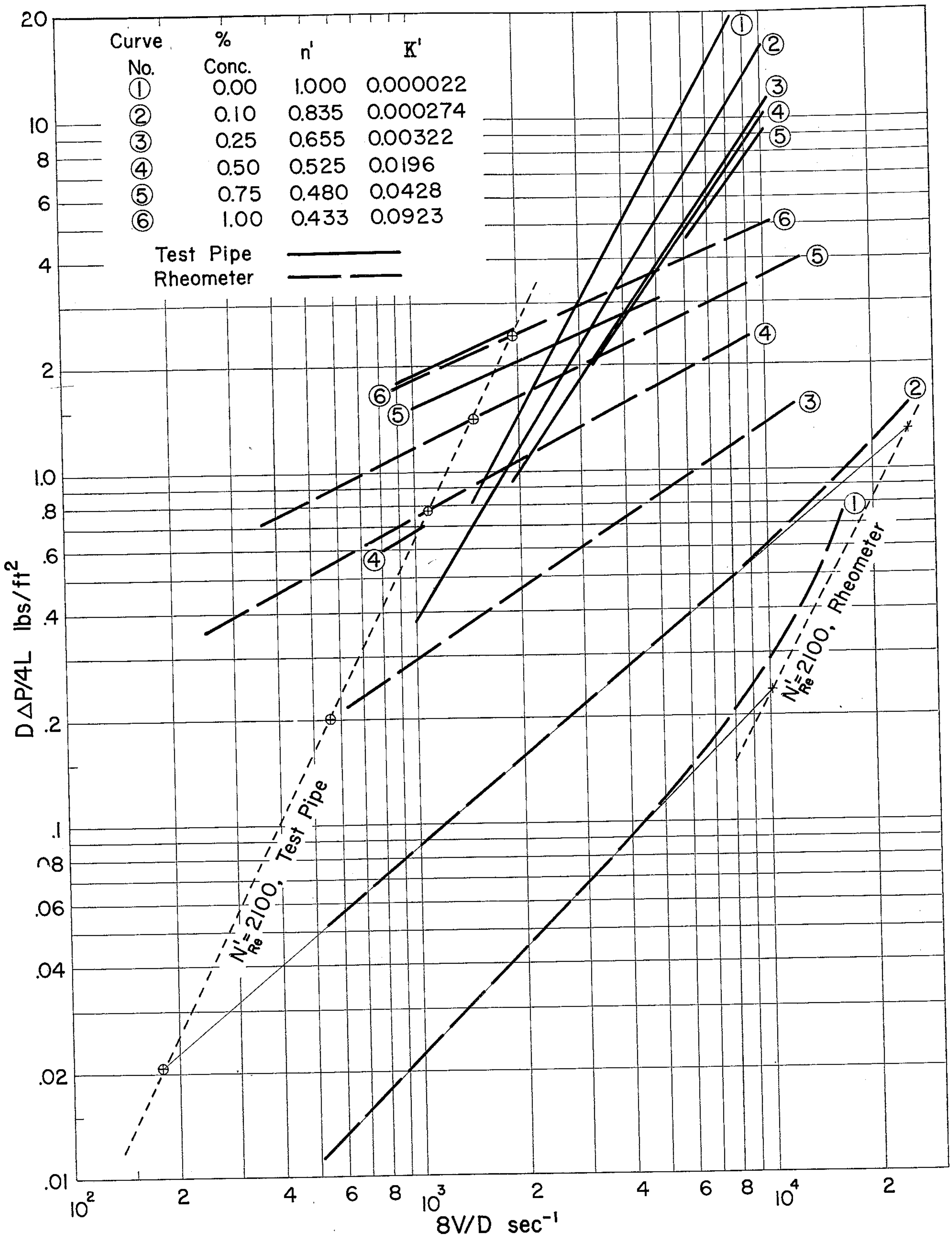

Fig. 9 - A Summary Shear Characterization for Various CMC Solutions at 70 F

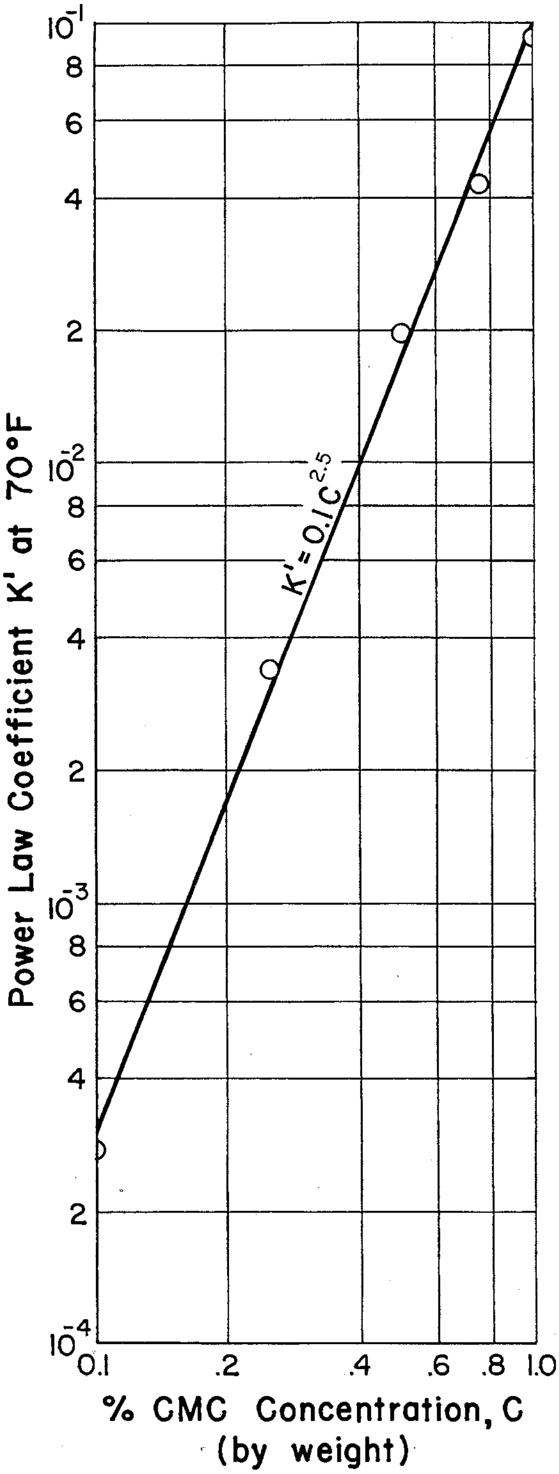

Fig. 11 - Effect of Concentration on the Power Law Coefficient K' for CMC Solutions at 70 F

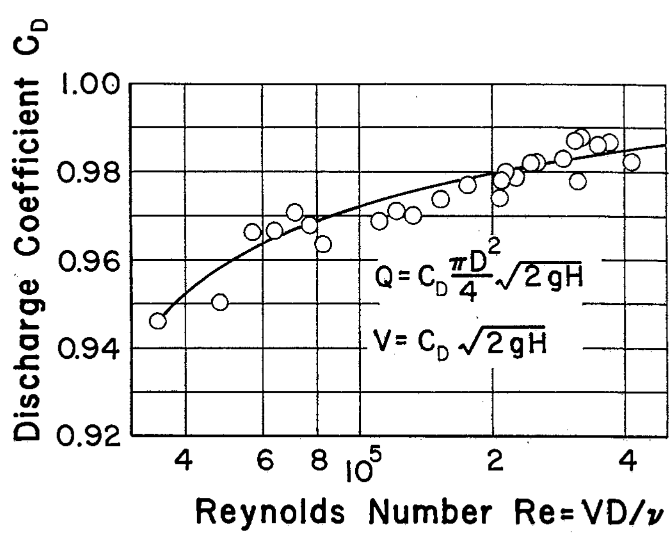

Fig. 12 - Fresh Water Calibration Curve for the Test Pipe Flow Meter

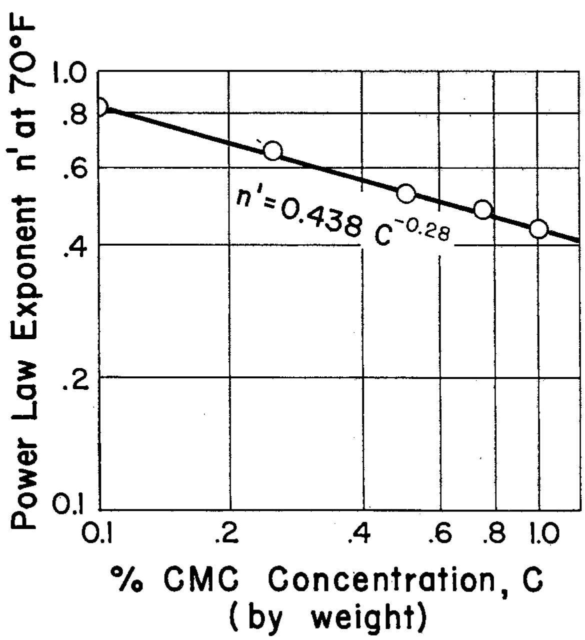

Fig. 10 - Effect of Concentration on the Power Law Exponent n' for CMC Solutions at 70 F

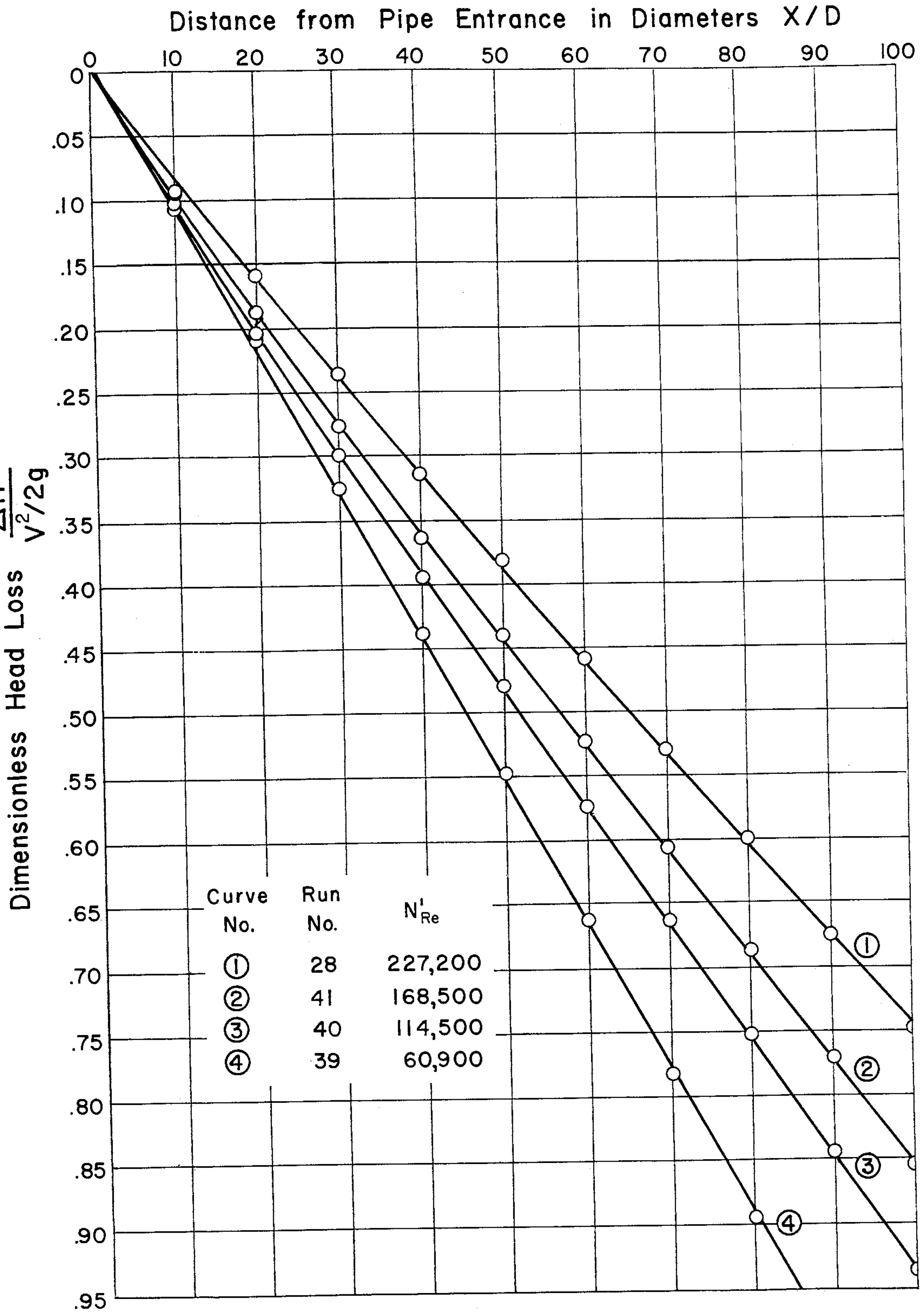

Fig. 13 - Hydraulic Gradients for the 0.10 per cent Solution at 70 F

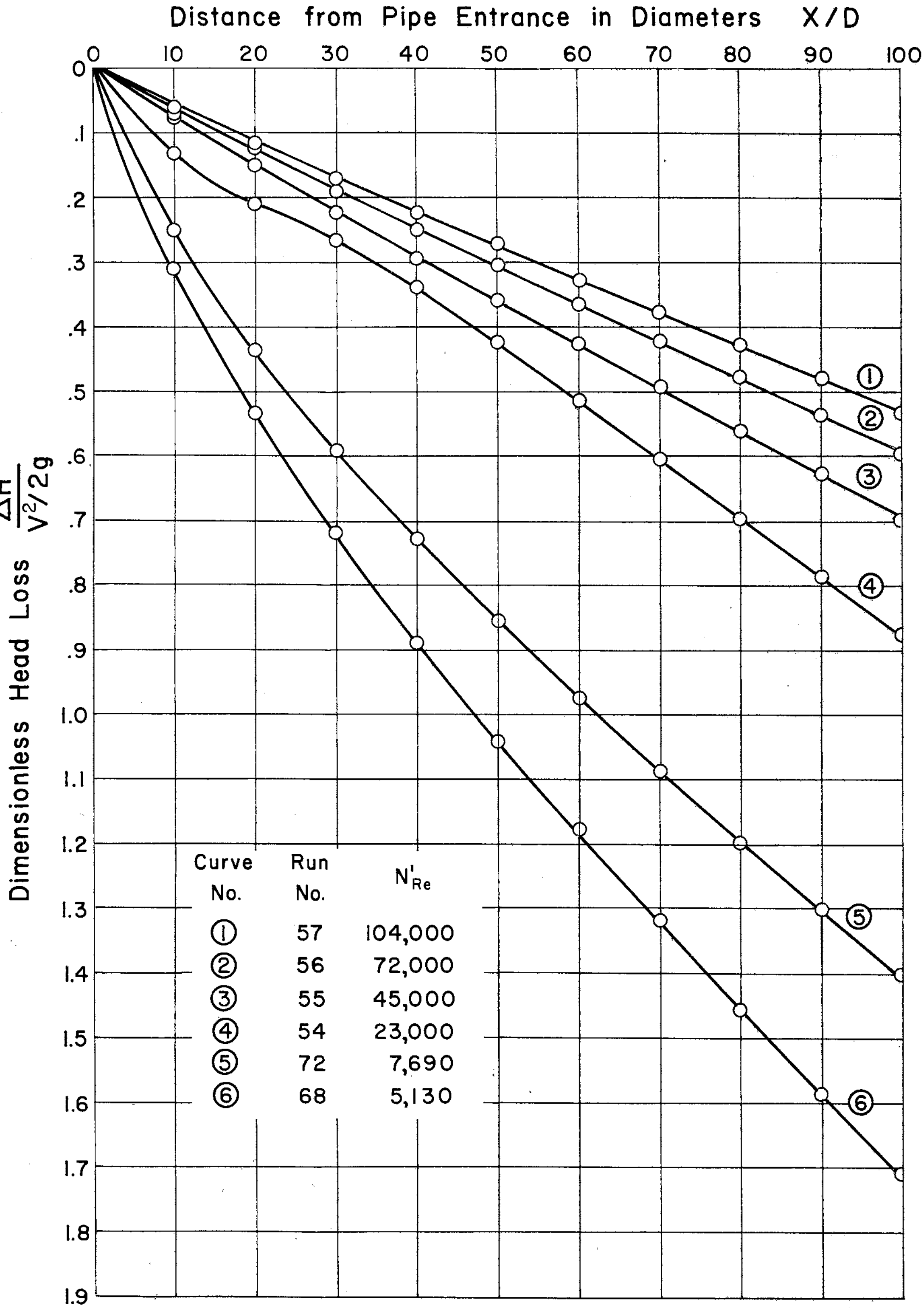

Fig. 14 - Hydraulic Gradients for the 0.25 per cent Solution at 70 F

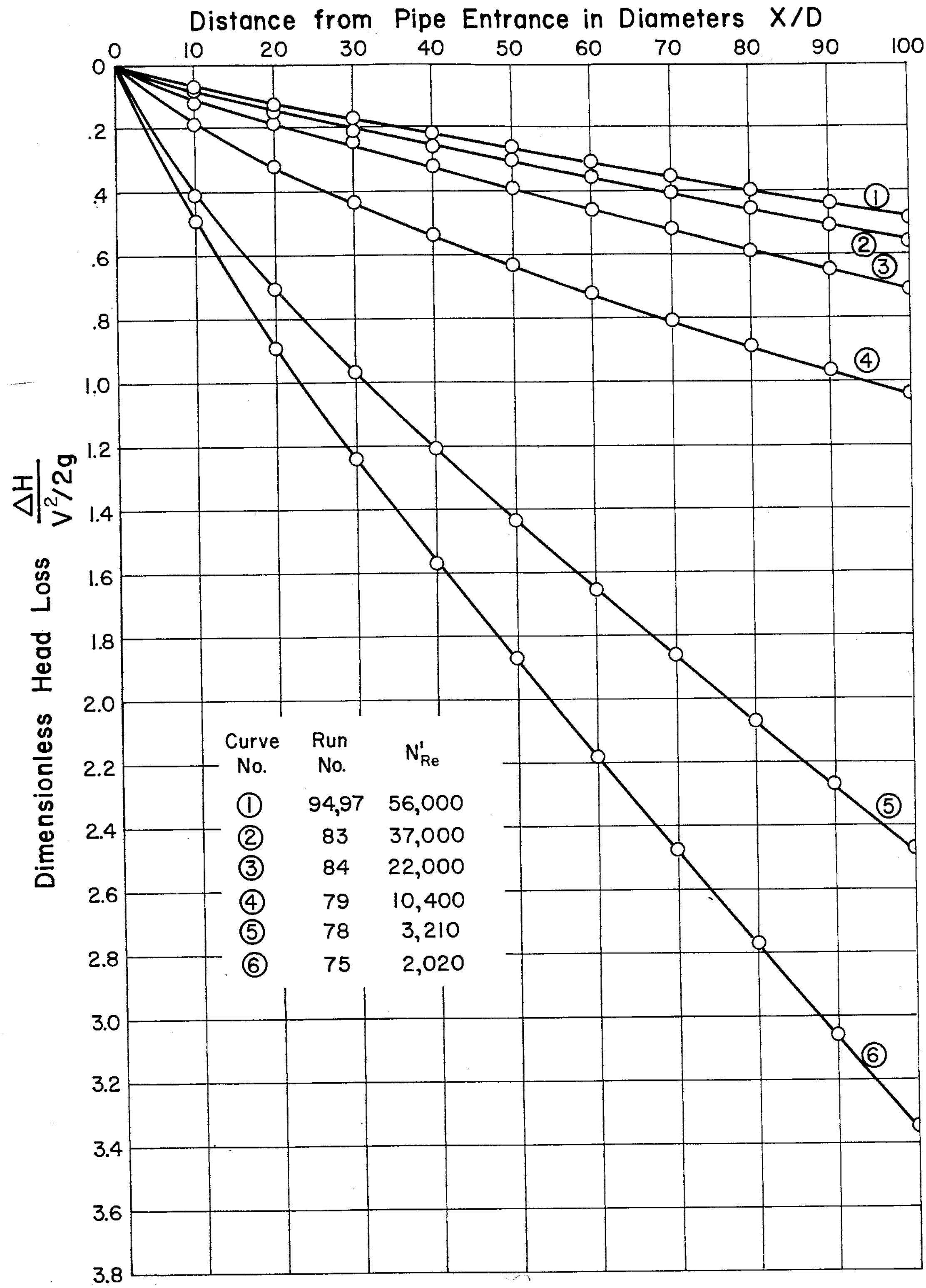

Fig. 15 - Hydraulic Gradients for the 0.50 per cent Solution at 70 F

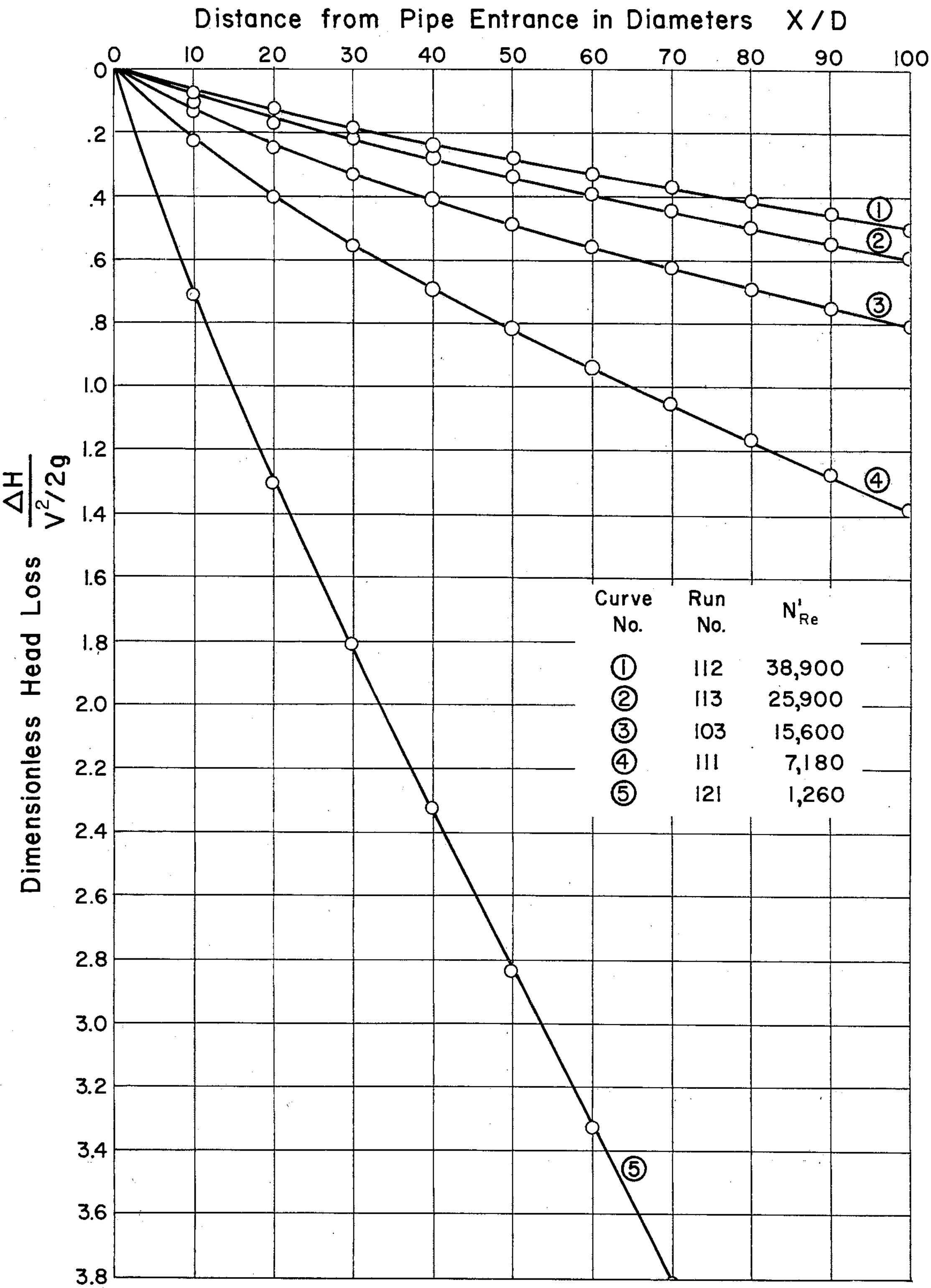

Fig. 16 - Hydraulic Gradients for the 0.75 per cent Solution at 70 F

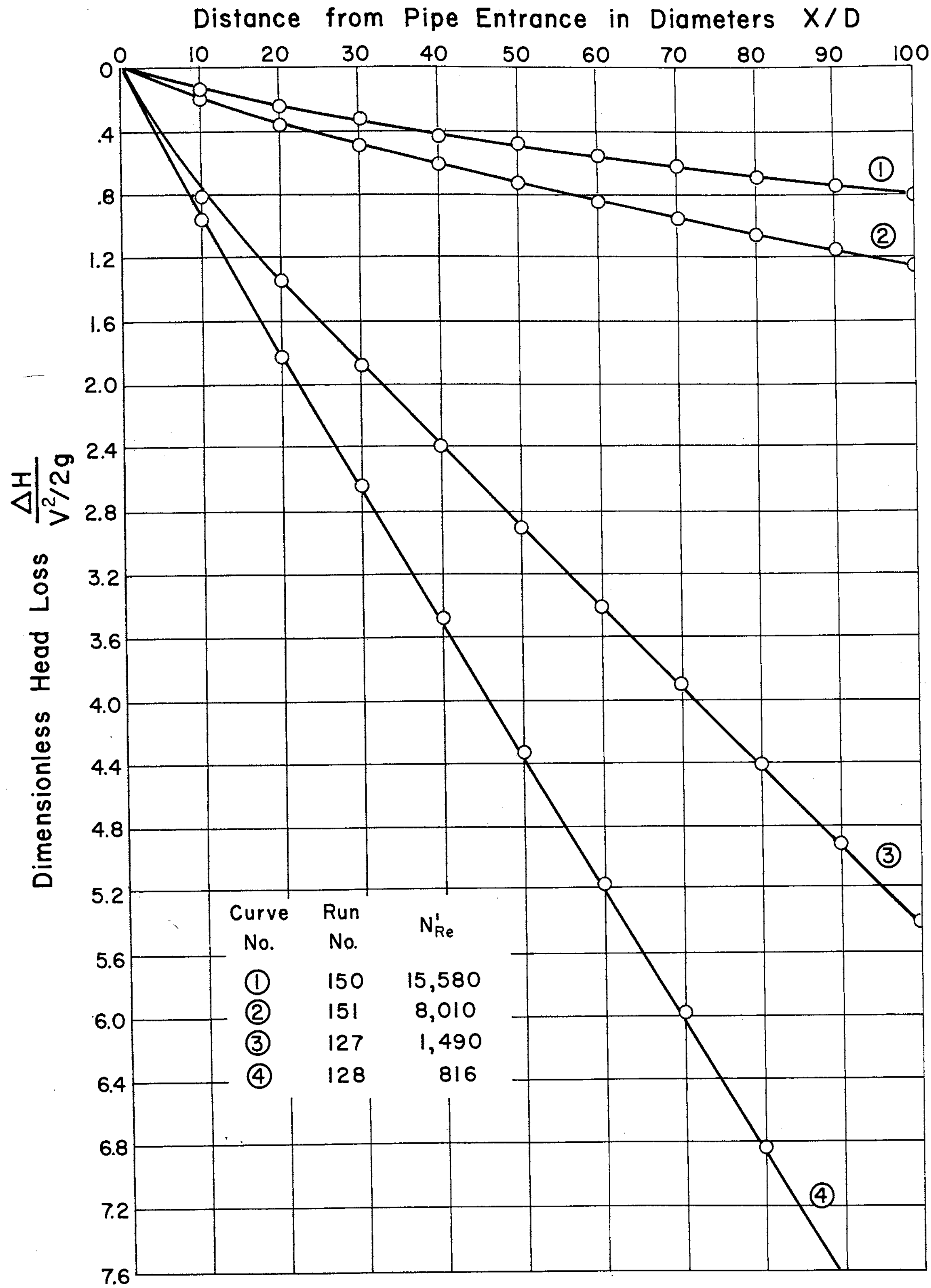

Fig. 17 - Hydraulic Gradients for the 1.00 per cent Solution at 70 F

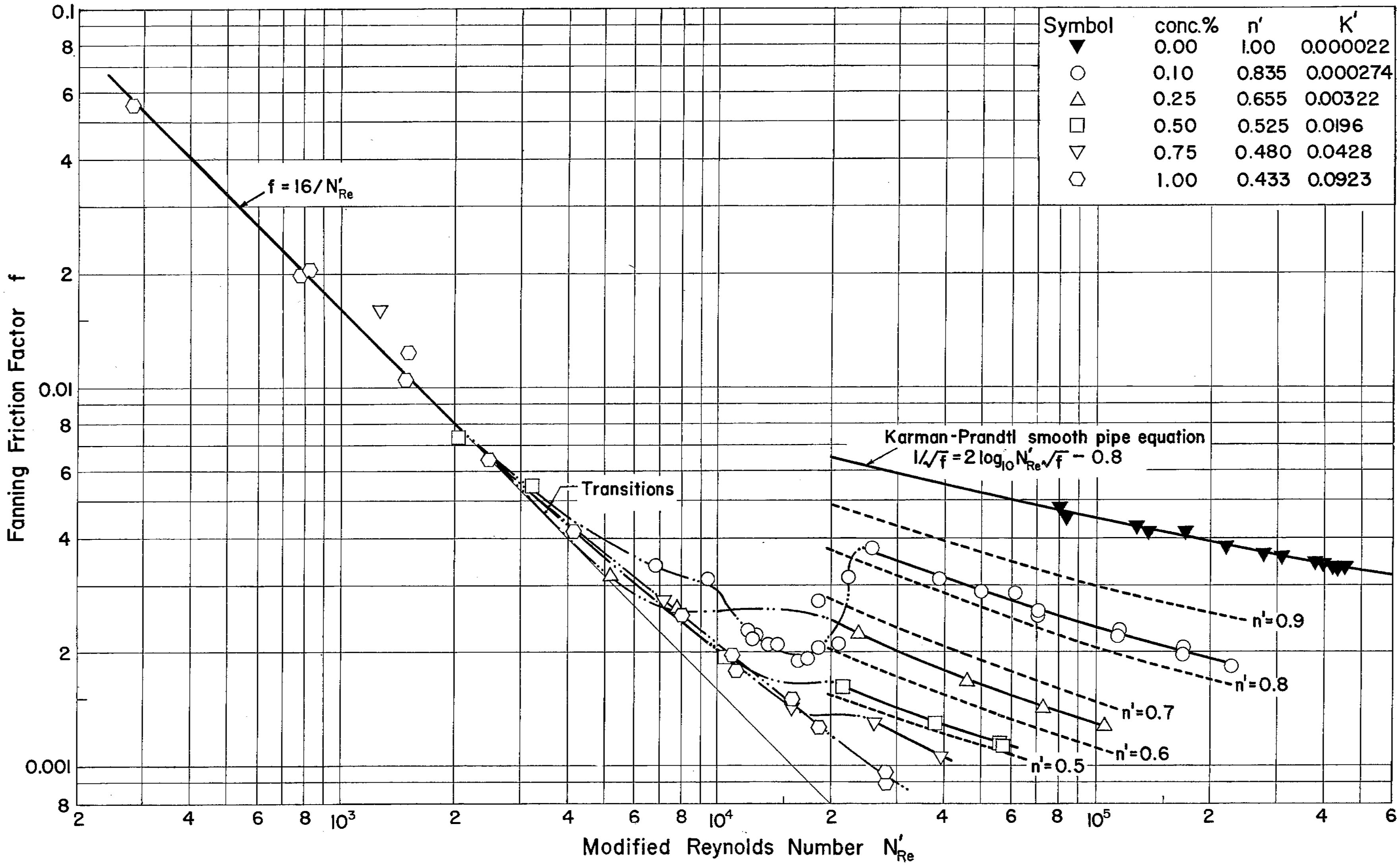

Fig. 18 – Friction factor, f, versus Reynolds Number, N'_{Re}, for a Smooth Pipe of 0.902-in. Diameter with Various CMC Solutions at 70 F

TABLE I - EXTRUSION RHEOMETER DATA (L = 51", D = 0.05")

Solution Conc. C (Per Cent)	Temp. (°F)	V (fps)	8V/D (sec^{-1})	$\frac{D \Delta P}{4L}$ (lbs/ft^2)	n'	K'
0.00	69.8	1.9289	3703	0.0842	1.00	0.0000220
	69.7	2.9456	5655	0.1387		
	69.6	4.5850	8803	0.2425		
	70.1	5.9923	11505	0.3550		
	69.5	6.8708	13192	0.4605		
	69.5	7.4990	14398	0.5869		
	69.5	8.3526	16037	0.7124		
	69.6	0.2810	540	0.0119		
	69.9	0.7985	1533	0.0334		
	69.7	1.3031	2502	0.0564		
	69.9	1.7927	3442	0.0783		
0.10	69.8	0.3294	632	0.0571	0.835	0.000274
	69.9	0.8025	1541	0.1246		
	69.7	0.9535	1831	0.1480		
	70.0	1.2329	2367	0.1780		
	69.6	1.7388	3338	0.2387		
	69.9	4.5027	8645	0.5306		
	69.9	7.1760	13778	0.8059		
	70.4	9.4463	18137	1.0795		
	70.5	11.2752	21648	1.2966		
	70.6	12.4819	23965	1.4218		
	85.3	6.6424	12753	0.6669	0.853	0.000200
	85.0	5.2633	10105	0.5265		
	85.5	3.7587	7217	0.3914		
	85.2	2.6841	5153	0.2887		
	85.0	1.6004	3073	0.1865		
	85.5	0.6330	1215	0.0847		
	100.0	7.6195	14630	0.6642	0.900	0.0001094
	100.0	6.1389	11785	0.5273		
	100.0	4.5568	8750	0.3914		
	100.+	2.8706	5510	0.2545		
	100.5	2.0376	3912	0.1856		
	100.5	1.4828	2847	0.1396		
	100.-	1.0492	2015	0.1016		
0.25	71.0	5.6547	10857	1.4079	0.655	0.00322
	70.4	3.6330	6975	1.0512		
	70.5	1.8728	3596	0.6914		
	70.5	0.3567	685	0.2305		

TABLE I (cont.)

Solution Conc. C (Per Cent)	Temp. (°F)	V (fps)	8V/D (sec^{-1})	$\frac{D \Delta P}{4L}$ (lbs/ft^2)	n'	K'
0.50	70.9	3.2595	6258	1.9355	0.525	0.0196
	70.5	1.7586	3377	1.4081		
	70.2	0.7118	1367	0.8708		
0.75	69.7	1.1061	2124	1.7654	0.480	0.0428
	69.7	2.0672	3969	2.2919		
	69.8	3.1394	6028	2.8142		
	69.9	4.9099	9427	3.4804		
	69.6	0.5597	1075	1.2257		
	70.3	0.2131	410	0.6968		
	70.4	0.2911	560	0.8711		
	70.8	0.9606	1844	1.5802		
1.00	69.6	0.2336	500	1.2579	0.433	0.0923
	70.0	0.4662	895	1.7589		
	70.1	0.8648	1660	2.2932		
	70.1	1.3880	2665	2.8152		
	70.1	2.2354	4292	3.4819		
	85.0	3.0064	5772	3.4740	0.506	0.04325
	85.0	1.9200	3686	2.8088		
	85.0	1.1344	2178	2.1157		
	85.0	0.4815	925	1.4049		
	85.2	0.6401	1229	1.5836		
	85.2	0.3965	761	1.2233		
	100.0	3.9846	7650	3.4655	Variable	Variable
	100.5	2.5546	4905	2.8017		
	100.0	1.4612	2805	2.1098		
	100.2	0.6707	1288	1.4001		
	100.2	0.4009	770	1.0039		

NOTE: The use of values carried to the fourth and fifth significant figure is a calculation and reference expedient rather than an indication of the accuracy of experimental procedures.

TABLE II - HYDRAULIC GRADIENT DATA AT 70°F

Solution Conc. C (Per Cent)	Run No.	V (fps)	N'_{Re}	Distance from Pipe Entrance in Diameters, X/D: 10	20	30	40	50	60	70	80	90	100
				Dimensionless Head Loss, $\frac{\Delta H}{V^2/2g}$									
0.10	39	30.26	60900	0.094	0.211	0.326	0.441	0.548	0.662	0.783	0.896	1.007	1.121
	40	52.03	114500	0.108	0.206	0.300	0.396	0.480	0.574	0.664	0.754	0.846	0.939
	41	72.50	168500	0.103	0.191	0.277	0.365	0.440	0.525	0.608	0.687	0.772	0.856
	28	93.67	227200	0.093	0.159	0.237	0.317	0.383	0.460	0.531	0.600	0.676	0.752
0.25	68	10.18	5130	0.314	0.536	0.723	0.892	1 046	1.182	1.322	1.459	1.590	1.715
	72	13.76	7690	0.255	0.440	0.594	0.732	0.858	0.977	1.091	1.201	1.304	1.406
	54	31.44	23400	0.137	0.215	0.271	0.341	0.426	0.517	0.607	0.697	0.786	0.876
	55	51.71	45600	0.082	0.155	0.227	0.297	0.361	0.430	0.496	0.563	0.630	0.699
	56	72.70	72200	0.071	0.134	0.195	0.255	0.308	0.368	0.425	0.481	0.538	0.597
	57	95.87	104700	0.064	0.120	0.175	0.229	0.276	0.330	0.380	0.430	0.480	0.533
0.50	75	9.99	2025	0.497	0.891	1.238	1.567	1.873	2.179	2.474	2.770	3.057	3.348
	78	13.66	3210	0.409	0.707	0.965	1.206	1.436	1.654	1.862	2.067	2.269	2.470
	79	31.01	10400	0.188	0.321	0.435	0.537	0.631	0.721	0.805	0.887	0.965	1.043
	84	51.57	22800	0.121	0.186	0.248	0.322	0.389	0.455	0.518	0.581	0.645	0.711
	83	72.67	37800	0.082	0.150	0.209	0.261	0.306	0.355	0.405	0.456	0.507	0.560
	94,97	95.51	56600	0.070	0.122	0.171	0.219	0.261	0.307	0.352	0.397	0.441	0.487
0.75	121	9.95	1260	0.724	1.309	1.814	2.331	2.840	3.329	3.819	4.311	4.803	5.273
	111	31.22	7180	0.238	0.411	0.559	0.695	0.821	0.942	1.057	1.169	1.278	1.386
	103	52.07	15600	0.147	0.252	0.341	0.421	0.494	0.564	0.631	0.695	0.756	0.813
	113	72.66	25900	0.109	0.181	0.223	0.283	0.341	0.398	0.451	0.502	0.552	0.606
	112	94.89	38900	0.083	0.137	0.192	0.244	0.288	0.333	0.375	0.418	0.460	0.506
1.00	128	9.97	816	0.964	1.835	2.645	3.482	4.332	5.167	5.987	6.828	7.674	8.475
	127	14.63	1490	0.832	1.352	1.887	2.403	2.908	3.411	3.911	4.410	4.913	5.412
	151	42.83	8010	0.208	0.365	0.500	0.621	0.737	0.846	0.952	1.055	1.155	1.255
	150	65.49	15580	0.148	0.250	0.337	0.417	0.486	0.557	0.622	0.685	0.747	0.806

TABLE III - SUMMARY SHEAR AND FRICTION DATA FOR THE 0.902-INCH TEST PIPE

Solution Conc. C (Per Cent)	Run No.	Temp. (°F)	V (fps)	Meas. Stations	Shear Rate 8V/D (sec^{-1})	Shear Stress D ΔP/4L (lbs/ft^2)	Modified Reynold's Number N'Re	Fanning Friction Factor f
0.00	2	54.0	14.01	7-11	1490	0.916	79500	0.00481
↑	6	58.0	14.43	7-11	1530	0.922	87000	0.00457
	3	57.2	21.35	7-11	2270	1.832	127000	0.00429
	7	59.8	22.21	7-11	2360	1.980	136000	0.00414
	8	60.8	27.39	7-11	2910	3.010	171000	0.00414
	9	61.0	35.23	7-11	3750	4.541	220000	0.00377
	11	55.6	47.41	7-11	5040	7.871	275000	0.00361
	10	53.8	54.23	7-11	5770	10.086	306000	0.00354
	13	61.0	60.17	7-11	6400	12.121	376000	0.00345
	12	63.3	65.35	7-11	6950	13.964	420000	0.00337
	15	54.9	69.58	7-11	7400	16.032	401000	0.00342
	18	55.6	72.47	7-11	7710	17.199	421000	0.00338
	17	54.8	74.82	7-11	7960	18.243	430000	0.00336
↓	16	52.8	76.99	7-11	8190	19.246	429000	0.00335
0.00	14	56.2	77.19	7-11	8220	19.205	452000	0.00333
0.10	186	69.7	4.63	9-10	495	0.070	6840	0.00338
↑	184	69.2	6.10	9-10	650	0.109	9430	0.00303
	194	69.8	7.48	9-10	795	0.130	11960	0.00239
	178	70.8	7.68	9-10	820	0.123	12300	0.00216
	195	69.8	7.87	9-10	840	0.132	12690	0.00221
	193	69.6	8.36	9-10	890	0.141	13610	0.00209
	185	69.4	8.79	9-10	935	0.156	14400	0.00208
	187	69.7	9.78	9-10	1040	0.174	16340	0.00188
	188	70.5	10.23	9-10	1090	0.197	17220	0.00195
	179	70.8	10.82	9-10	1150	{0.228 / 0.306}	18400	{0.00201 / 0.00270}
	189	70.5	12.09	9-10	1290	{0.296 / 0.332}	20910	{0.00209 / 0.00235}
	191	70.7	12.71	9-10	1350	{0.478 / 0.602}	22180	{0.00306 / 0.00388}
	190	70.5	13.21	9-10	1405	0.659	23200	0.00390
	183	69.5	14.17	9-10	1510	0.732	25400	0.00377
	180	70.6	20.33	9-10	2160	1.243	38300	0.00311
	182	69.3	25.29	8-9	2690	1.797	49400	0.00291
	39	69.6	30.26	7-11	3220	2.537	60900	0.00286
	181	71.0	34.14	8-9	3635	2.810	70100	0.00249
	192	69.5	34.18	8-9	3640	2.898	70200	0.00256
	26	70.0	51.67	7-11	5500	5.683	113600	0.00220
	40	69.6	52.03	7-11	5540	5.979	114500	0.00228
	41	69.7	72.50	7-11	7715	10.525	168500	0.00207
↓	27	69.7	72.58	7-11	7725	10.078	168800	0.00198
0.10	28	70.1	93.67	7-11	9970	15.515	227200	0.00193

TABLE III (cont.)

Solution Conc. C (Per Cent)	Run No.	Temp. (°F)	V (fps)	Meas. Stations	Shear Rate 8V/D (sec^{-1})	Shear Stress D ΔP/4L (lbs/ft^2)	Modified Reynold's Number N'_{Re}	Fanning Friction Factor f
0.10	202	84.3	4.45	9-10	475	0.052	8090	0.00270
	208	85.2	5.59	9-10	595	0.076	10500	0.00253
	207	85.0	6.26	9-10	670	0.084	11950	0.00223
	203	84.0	6.90	9-10	735	0.092	13400	0.00200
	201	85.3	7.81	9-10	830	0.123	15400	0.00209
	206	84.7	8.45	9-10	900	{0.145, 0.290}	16800	0.00211
	205	84.7	9.40	9-10	1000	{0.238, 0.388}	19100	0.00279
	204	84.5	11.20	9-10	1190	0.535	23300	0.00442
	200	85.5	11.31	9-10	1205	0.523	23600	0.00423
	199	85.5	14.65	9-10	1560	0.805	31700	0.00389
	198	85.2	19.46	9-10	2070	1.155	43900	0.00316
	197	84.3	26.68	8- 9	2840	1.932	63000	0.00281
	42	85.2	31.17	7-11	3315	2.570	75400	0.00274
	196	84.7	34.18	8- 9	3640	2.867	83800	0.00254
	43	85.0	51.65	7-11	5495	5.831	134500	0.00226
	30	84.7	51.75	7-11	5510	5.712	134800	0.00221
	31	85.0	72.69	7-11	7735	10.077	199000	0.00197
	44	84.6	72.71	7-11	7740	10.339	199100	0.00204
	32	85.3	92.63	7-11	9860	15.238	262800	0.00184
	213	100.6	4.60	9-10	490	0.054	11300	0.00266
	212	100.6	9.32	9-10	990	{0.274, 0.377}	24600	0.00327
	211	99.7	12.11	9-10	1290	0.598	32800	0.00424
	210	100.3	13.41	9-10	1425	0.703	36700	0.00406
	47	99.3	30.80	7-11	3280	2.485	91600	0.00272
	209	100.8	33.50	8- 9	3565	2.934	100400	0.00271
	33	99.8	50.24	7-11	5350	5.575	157000	0.00230
	46	100.3	51.86	7-11	5520	5.778	162000	0.00223
	34	99.6	72.75	7-11	7745	10.031	236000	0.00197
	45	100.0	72.89	7-11	7760	10.221	236000	0.00200
0.10	35	100.3	92.72	7-11	9870	15.118	308000	0.00183
0.25	68	71.1	10.18	9-11	1085	0.321	5130	0.00320
	72	68.2	13.76	9-11	1465	0.471	7690	0.00257
	54	70.0	31.44	7-11	3345	2.145	23400	0.00224
	55	69.6	51.71	7-11	5035	4.352	45600	0.00168
	56	69.5	72.70	7-11	7735	7.311	72200	0.00143
0.25	57	69.4	95.87	7-11	10200	11.331	104700	0.00127

TABLE III (cont.)

Solution Conc. C (Per Cent)	Run No.	Temp. (°F)	V (fps)	Meas. Stations	Shear Rate 8V/D (sec^{-1})	Shear Stress D ΔP/4L (lbs/ft^2)	Modified Reynold's Number N'_{Re}	Fanning Friction Factor f
0.25	69	85.4	10.28	9-11	1095	0.293		
	73	85.8	13.73	9-11	1460	0.414		
	61	85.2	31.74	7-11	3380	2.153		
	60	84.9	51.55	7-11	5485	4.338		
	59	84.7	72.56	7-11	7720	7.252		
	58	85.4	96.23	7-11	10240	11.271		
	70	101.1	10.22	9-11	1090	0.267		
	74	97.2	13.82	9-11	1470	0.389		
	71	99.6	14.33	9-11	1525	0.396		
	62	100.2	30.96	7-11	3300	2.148		
	63	99.5	51.67	7-11	5500	4.434		
	64	99.4	72.81	7-11	7750	7.655		
0.25	65	99.8	94.23	7-11	10030	11.443		
0.50	75	71.0	9.99	7-11	1065	0.705	2025	0.00731
	78	69.9	13.66	9-11	1455	0.911	3210	0.00544
	79	71.6	31.01	9-11	3300	1.810	10400	0.00194
	84	70.2	51.57	9-11	5490	4.182	22800	0.00162
	83	69.8	72.67	9-11	7735	6.650	37800	0.00130
	97	70.2	95.17	9-11	10130	10.048	56300	0.00115
	94	71.8	95.85	9-11	10200	10.052	56900	0.00113
	76	84.7	9.99	7-11	1065	0.634		
	88	85.0	13.82	9-11	1470	0.796		
	87	84.7	31.42	9-11	3345	1.762		
	85	84.9	51.66	9-11	5500	4.262		
	86	85.1	72.66	9-11	7735	6.687		
	95	84.8	94.37	9-11	10050	10.058		
	77	99.9	10.04	7-11	1070	0.562		
	89	99.8	13.70	9-11	1460	0.731		
	90	100.0	31.17	9-11	3315	1.637		
	91	100.0	51.88	9-11	5520	4.358		
	92	99.4	72.75	9-11	7745	6.815		
0.50	96	99.7	93.22	9-11	9920	10.121		

TABLE III (cont.)

Solution Conc. C. (Per Cent)	Run No.	Temp. (°F)	V (fps)	Meas. Stations	Shear Rate 8V/D (sec^{-1})	Shear Stress $D\Delta P/4L$ (lbs/ft^2)	Modified Reynold's Number N'_{Re}	Fanning Friction Factor f
0.79	121	70.6	9.95	7-10	1060	1.553	1260	0.01620
	111	71.3	31.22	8-11	3325	2.582	7180	0.00274
	103	70.9	52.07	10-11	5540	3.733	15600	0.00142
	113	71.8	72.66	7-11	7735	6.611	25900	0.00130
	112	70.6	94.89	7-10	10100	9.238	38900	0.00106
	117	85.9	9.42	7-10	1000	1.424		
	114	86.1	31.48	8-11	3350	2.433		
	104	84.8	52.35	10-11	5570	3.599		
	105	85.0	72.69	8-10	7735	6.485		
	106	85.2	94.57	7-10	10065	9.404		
	118	101.1	9.45	7-10	1005	1.235		
	109	100.2	31.17	8-11	3315	2.259		
	101	100.0	51.79	10-11	5510	2.935		
	108	99.8	73.07	7-10	7775	6.839		
0.75	107	99.7	95.02	8-11	10115	9.993		
1.00	164	69.5	5.00	7-11	530	1.329	276	0.05505
	162	69.0	9.65	9-10	1030	1.803	775	0.02004
	128	72.2	9.97	7-11	1060	1.987	816	0.02067
	163	69.7	14.55	9-10	1550	2.158	1480	0.01053
	127	70.9	14.63	7-11	1555	2.588	1490	0.01251
	145	69.7	20.07	9-10	2135	2.536	2440	0.00650
	151	69.3	42.83	9-11	4560	4.442	8010	0.00250
	135	70.6	52.05	9-10	5540	5.163	10870	0.00197
	134	69.3	52.93	9-10	5635	4.847	11160	0.00179
	150	69.2	65.49	9-11	6970	6.259	15580	0.00151
	136	72.5	73.12	9-10	7780	6.579	18520	0.00127
	138	71.0	94.92	9-10	10100	8.251	27870	0.00947
	137	72.5	95.36	9-10	10150	8.224	28080	0.00909
	123	84.0	14.53	7-11	1545	2.254	1830	0.00875
	149	85.3	20.11	9-10	2140	2.728	2980	0.00698
	125	86.2	32.00	7-11	3400	3.443	5970	0.00348
	154	85.9	38.63	9-11	4110	3.883	7900	0.00269
	147	84.1	41.02	9-10	4365	4.143	8650	0.00255
1.00	130	84.3	50.54	9-10	5380	4.875	11810	0.00197

TABLE III (cont.)

Solution Conc. C. (Per Cent)	Run No.	Temp. (°F)	V (fps)	Meas. Stations	Shear Rate 8V/D (sec-1)	Shear Stress D ΔP/4L (lbs/ft2)	Modified Reynold's Number N'Re	Fanning Friction Factor f
1.00	131	85.1	52.16	9-10	5550	4.925	12380	0.00187
↑	153	84.4	58.96	9-11	6275	5.879	14880	0.00175
	148	84.5	60.25	9-10	6410	5.354	15360	0.00153
	132	86.1	72.74	9-10	7740	6.439	20350	0.00126
	139	84.7	95.01	9-10	10110	7.956	30340	0.00091
	133	86.9	95.18	9-10	10130	7.776	30410	0.00089
	168	99.5	6.25	7-11	665	1.262		
	161	100.0	9.28	9-10	990	1.520		
	160	99.6	15.05	9-10	1600	2.040		
	159	101.0	20.29	9-10	2160	2.241		
	167	100.2	28.29	7-11	3010	2.966		
	166	99.0	29.05	7-11	3090	2.877		
	158	99.4	30.83	10-11	3280	2.860		
	165	100.1	31.02	7-11	3300	3.015		
	143	102.5	31.70	7-11	3375	3.173		
	157	100.8	44.58	9-11	4745	4.117		
	142	99.5	52.11	9-10	5545	4.723		
	156	99.8	72.82	9-11	7750	6.424		
	141	99.6	72.85	9-10	7755	6.096		
	170	100.1	78.19	9-10	8320	7.205		
	171	100.0	87.86	9-10	9350	8.283		
	155	99.6	95.12	7-11	10125	9.088		
↓	140	99.2	95.41	9-10	10155	8.176		
1.00	172	100.0	101.94	9-10	10850	9.792		

NOTE: The use of values carried to the fourth and fifth significant figure is a calculation and reference expedient rather than an indication of the accuracy of experimental procedures.

DISTRIBUTION LIST FOR TECHNICAL PAPER NO. 42-B

Copies	Organization
65	Commanding Officer and Director, David Taylor Model Basin, Washington 7, D. C., Attn: Code 513.
9	Chief, Bureau of Ships 3 - Technical Library 1 - Preliminary Design (Code 420) 1 - Hull Design (Code 440) Development 1 - Research and Planning (Code 330) 1 - (Code 341B) HYDROMECHANICS, LOGISTICS, and SPECIAL CRAFT 1 - (Code 345) SHIP SILENCING 1 - LABORATORY MANAGEMENT DIVISION (Code 320)
6	Chief, Bureau of Yards and Docks, Department of the Navy, Washington 25, D. C.
6	Chief, Bureau of Naval Weapons, Department of the Navy, Washington 25, D. C., Attn: Underwater Ordnance (Code Re6a). 3 - RU 3 - RAAD
3	Chief of Naval Research, Department of the Navy, Washington 25, D. C. 3 - Fluid Dynamics Branch (Code ONR 438).
1	Director, U. S. Naval Research Laboratory, Washington 25, D. C., Attn: Code 2021.
1	Commanding Officer, Office of Naval Research, Branch Office, 230 N. Michigan Avenue, Chicago 1, Illinois.
1	Commander, U. S. Naval Ordnance Laboratory, White Oak, Silver Spring, Maryland.
2	Commander, U. S. Naval Ordnance Test Station, 3202 East Foothill Boulevard, Pasadena, California. 1 - Mr. A. G. Fabula
1	Commanding Officer and Director, U. S. Navy Underwater Sound Laboratory, Fort Trumbull, New London, Connecticut.
2	Director, Ordnance Research Laboratory, Pennsylvania State University, University Park, Pennsylvania.
1	Superintendent, U. S. Naval Postgraduate School, Monterey, California, Attn: Librarian.
1	Assistant Secretary of the Army, (Research and Development), Department of the Army, Washington 25, D. C.

Copies	Organization
1	Director, U. S. Waterways Experiment Station, Corps of Engineers, P. O. Box 631, Vicksburg, Mississippi, Attn: Technical Librarian.
1	Office of the Chief of Engineers, Civil Works, Department of the Army, Gravelly Point, Washington 25, D. C.
1	Director of Research, National Aeronautics and Space Administration, 1520 H. Street, N. W., Washington 25, D. C.
1	Director, Langley Aeronautical Laboratory, National Aeronautics and Space Administration, Langley Field, Virginia.
1	Director, Hydraulic Laboratory, Bureau of Reclamation, Denver Federal Center, Denver, Colorado.
20	Defense Documentation Center for Scientific and Technical Information, Arlington Hall Station, Arlington 12, Virginia.
2	Director, National Bureau of Standards, National Hydraulic Laboratory, Washington 25, D. C.
2	Newport News Shipbuilding and Dry Dock Company, Newport News, Virginia. For distribution as follows: 1 - ASST. Naval Architect 1 - Director, Hydraulic Laboratory
1	California Institute of Technology, Division of Engineering, Pasadena 4, California.
2	Director, Davidson Laboratory, Stevens Institute of Technology, 711 Hudson Street, Hoboken, New Jersey.
1	Director, Hydraulic Laboratory, Worcester Polytechnic Institute, Worcester 2, Massachusetts.
1	Director, Hydrodynamics Laboratory, Massachusetts Institute of Technology, Cambridge 39, Massachusetts.
1	Head, Department of Naval Architecture and Marine Engineering, Massachusetts Institute of Technology, Cambridge 39, Massachusetts.
1	Director, Woods Hole Oceanographic Institute, Woods Hole, Massachusetts.
1	Director, Iowa Institute of Hydraulic Research, State University of Iowa, Iowa City, Iowa.
1	Hydronautics, Incorporated, Pindell School Road, Laurel, Maryland, Attn: Mr. Phillip Eisenberg.
1	Western Co. of North America, 1171 Empire Central, Dallas 7, Texas, Attn: Dr. H. R. Crawford.

Copies	Organization
1	Department of Chemical Engineering, University of Delaware, Newark, Delaware, Attn: Dr. A. B. Metzner.
1	Director, Engineering Societies Library, 29 West 39th Street, New York 18, New York.
2	Library, California Institute of Technology, Pasadena, California.
1	Librarian, Massachusetts Institute of Technology, Cambridge 39, Massachusetts.
1	Librarian, School of Engineering, University of Texas, Austin, Texas.
3	Serials Division, University of Minnesota Library, Minneapolis, Minnesota.